2020

The Effects of an Inflammasome Inhibitor OLT1177 on the Development of Ischemic Heart Failure

Joseph S. Aliaga
Virginia Commonwealth University

Downloaded from
https://scholarscompass.vcu.edu/etd/6326

COPYRIGHT PAGE

**THE EFFECTS OF AN INFLAMMASOME INHIBITOR OLT1177 ON THE
DEVELOPMENT OF ISCHEMIC HEART FAILURE**

A thesis submitted in partial fulfillment of the requirements for the degree of Master of Science

in Physiology and Biophysics at Virginia Commonwealth University.

By

Joseph Aliaga, BS

Directors:

Antonio Abbate, MD PhD, Stefano Toldo PhD

Virginia Commonwealth University

Richmond, Virginia

May, 2020

Acknowledgement

Table of Contents

List of Tables

List of Figures

Thesis Abstract

THE EFFECTS OF AN INFLAMMASOME INHIBITOR OLT1177 ON THE DEVELOPMENT OF ISCHEMIC HEART FAILURE

By Joseph S. Aliaga, BS

A thesis submitted in partial fulfillment of the requirements for the degree of Master of Science at Virginia Commonwealth University.

Virginia Commonwealth University, 2020

Background: Evidence suggests that prolonged and enhanced pro-inflammatory signaling, modulated by the NLRP3 inflammasome, plays a crucial role in the pathophysiology of several different types of cardiovascular diseases such as acute myocardial infarction (AMI), adverse ventricular remodeling, and heart failure (HF). Consequently, we hypothesize that attenuating the enhanced inflammatory response using a pharmacological NLRP3 inflammasome inhibitor would decrease cell death, improve cardiac function, limit adverse cardiac remodeling, and overall reduce the risk of developing ischemic heart failure. We investigated the role of the NLRP3 inflammasome after a nonreperfused AMI, by studying the effects of inhibiting the NLRP3 inflammasome.

Methods: In this study we used a mouse model of acute myocardial infarction (AMI) due to permanent coronary artery ligation. We assessed cardiac function in mice using transthoracic echocardiography 3 days after inducing a large nonreperfused AMI, via permanent ligation of the LAD coronary artery, and select mice with large nonreperfused anterior infarct (≥ 4 akinetic segments involving the anterior wall) as well as an enlarged ventricle (left ventricular end-

diastolic diameter [LVEDD] $\geq$ 4.4 mm) and systolic dysfunction (left ventricular ejection fraction [LVEF] $\leq$ 40%). The mice were then randomly assigned to one of four groups. Group 1 (n=8) consisted of mice with an AMI and were fed OLT1177, a NLRP3 inflammasome inhibitor admixed with the chow in the diet (3.75 gr/kg) for 10 weeks. Group 2 (n=7) consisted of mice with an AMI and were fed OLT1177, a NLRP3 inflammasome inhibitor admixed with the chow in the diet (7.5 gr/kg) for 10 weeks. Group 3 (n=7) consisted of mice with AMI that were fed a standard diet (without OLT1177) for 10 weeks. Group 4 (n=6) consisted of mice that underwent a sham operation and had no AMI and were fed a standard diet for 10 weeks. We repeated transthoracic echocardiography assessments 4-weeks and 10-weeks after coronary artery ligation surgery with an assessment of changes in LVEF, along with isoproterenol challenge in order to measure contractile reserve, a surrogate for cardiorespiratory fitness. The surviving mice underwent LV catheterization, a terminal procedure, in order to evaluate left ventricular diastolic function in vivo by measuring left ventricular end-diastolic pressure.

Results: At the end of 10 weeks, 2 of 10 mice (20%) had died in OLT 3.75 gr/kg group, as compared with 2 of 9 (22%) in the OLT 7.50 gr/kg group, 3 of 10 mice (30%) in the control diet group, and 0 of 6 mice (0%) in the sham-operated group. Treatment with OLT 3.75 gr/kg or 7.50 gr/kg led to preservation of contractile reserve (percent increase in LVEF after isoproterenol challenge [+33±11% or +40±6% vs +9±7 % in standard diet; P<0.05 and P<0.005 respectively). Treatment with OLT 3.75 gr/kg or 7.5 gr/kg also led to preservation of diastolic function (left ventricular end-diastolic pressure 3.2±0.5 mmHg, or 4.5±0.5 mmHg vs 10.0±1.6 mmHg in standard diet; P<0.005 and P<0.009). These effects were independent of effects on ventricular remodeling after AMI.

Conclusions/implications: The results presented in this study show that NLRP3 inhibition with OLT1177 can preserve ß-adrenergic responsiveness and prevent left ventricular diastolic dysfunction in large nonreperfused anterior AMI thereby reducing the risk of developing post-infarct heart failure.

Keywords: Acute myocardial infarction, cardiac remodeling, heart failure, NLRP3 inflammasome, NLRP3 inflammasome inhibitor, OLT1177

Thesis Introduction

This thesis document has been organized to include a relevant review of background information regarding acute myocardial infarction, ventricular remodeling, and heart failure. An overview is also presented on the physiological processes that follow a myocardial infarction that occurs in an inflammatory response mediated by the NLRP3 inflammasome. Lastly, this article provides a brief overview of a novel inflammasome inhibitor (OLT1177) and discusses its potential use as a pharmacological intervention targeting inflammation in a nonreperfused AMI murine model study.

CHAPTER 1: Motivation and Significance

1.1 Background

The American Heart Association approximates that every 40 seconds, an American has a heart attack (MI). Correspondingly, the number of acute myocardial infarctions is rising, and as a result has become one of the most prevalent causes of hospitalization and death in the United States (Benjamin et al., 2019). Even so, thanks to medical advancements, and the continuous improvement in effective and prompt medical treatment, patients are surviving and living longer after a myocardial infarction(s). However, just as more people are living longer after an MI, there has been a continuous rise in the prevalence of post-MI heart failure (Benjamin et al., 2019)

According to current scientific literature, infarcted myocardium in most patients can be salvaged if coronary arterial flow and patency is restored promptly (Cohen et al., 2010). Conversely, evidence-based findings show that if treatment is delayed, myocardial infarct size or rate of myocardial cell death/injury increases resulting in a higher risk of developing a maladaptive form of cardiac remodeling that is mediated by neurohormonal and inflammatory signaling pathways. This form of adverse cardiac remodeling is one of many factors that over time contributes to the risk of developing post-MI heart failure, both for short-term and extended periods of time (Azevedo et al., 2016). For this reason, therapies developed in the last 20 years, such as those that target neurohormonal signaling pathways, and current/novel therapies that are targeting inflammatory signaling pathways are being developed and continually improved upon with the intent of preventing adverse cardiac remodeling and heart failure (Bhatt et al., 2017).

1.1.1 Acute Myocardial Infarction (AMI)

Under normal physiological conditions, the heart's atria and ventricles work in unison to carry out the hearts main function – pumping blood in a unidirectional manner throughout the body. This highly coordinated, continuous, and life-long form of perfusion is controlled by the heart's conduction system consisting of myogenic (spontaneous contraction initiated by the heart) electrical impulses that begin at the sinoatrial (SA) node located in the right atrium. This impulse next spreads throughout the walls of both right and left atria, then to the atrioventricular (AV) node, AV bundle, and to the rest of the Purkinje muscle fibers in right and left ventricles. Once these ventricle chambers receive the impulse myocardial cells contract, creating a pressure that is capable of opening heart valves and pumping blood through the pulmonary artery and to the lungs for blood oxygenation, as well as through the aorta and arterial circulation; whereby the body's muscles and tissues, including the heart's myocardium via coronary arteries, receives oxygenated blood and nutrients.

Although the SA node works as the "heart's natural pacemaker" capable of affecting and altering heart rate, blood pressure, contractility, and coronary artery flow; there are other factors that also play a role in regulation. These factors include nerve impulses from the autonomic nervous system (parasympathetic and sympathetic) and neurohormonal effects regulated by the sympathetic nervous system (SNS) and the renin-angiotensin-aldosterone system (RAAS). Together in a dynamic manner, the heart's conduction system, autonomic nervous system, and neurohormonal effects help create a balance between the heart's O_2 demand and O_2 supply.

An instance when this balance is altered, occurs when a coronary artery is partially or completely occluded resulting in a decrease of O_2 supply to the myocardium (ischemia) that can eventually lead to an acute myocardial infarction (AMI). Furthermore, the occlusion of a

coronary artery can swiftly lead to ischemic injury, and the impairment of myocardial metabolism (decreased cellular ATP levels) resulting in cell swelling and necrotic cell death in the ischemic area, and apoptosis in the ischemic tissue, the surrounding border zone, and non-ischemic myocardial area (Abbate et al., 2002).

A key feature of cell death during an AMI is that it progresses in the left ventricle wall from the subendocardium toward the myocardium and epicardium in a transmural manner (M. Tanaka, V. Richard, C. Murry, R. Jennings, Reimer, 1993). The reasons for this cell death progression are due to the subendocardium being subjected to the highest pressure coming from the ventricular chamber filled with blood, having fewer collateral blood vessel connections, and to being perfused by coronary arteries that must first reach and pass through layers of contracting myocardium (Lilly, 2013). Additionally, cardiac tissue that is directly supplied by an occluded coronary artery will die quickly, whereas tissue adjacent to the myocardial infarct can survive temporarily under ischemic conditions, due to collateral vessels from neighboring non-occluded coronary arteries. Nevertheless, as more time passes under ischemic conditions, tissue adjacent to the myocardial infarct will unavoidably succumb to infarction/necrotic cell death (Lilly, 2013). Together, the prolongation and severity of ischemia, impairment of myocardial metabolism, and necrotic cell death will lead to a cascade of events such as acute inflammation and immune cell recruitment which further increases cell death, inflammatory signaling, and loss of cardiac function. Additionally, characteristic AMI symptoms do occur in the form of systolic/diastolic dysfunction, arrhythmia, chest pain, shortness of breath, changes in protein levels (cTnI, cTnT, and CK-MB) proportional to the amount of cardiac tissue that is damaged, and the inflammatory responses to the myocardial injury (Pandey et al., 2020).

1.1.2 Diagnosis of Acute Myocardial Infarction (AMI)

While there exist various subtypes of myocardial infarction related to its causes, the two most prevalent types are type I and type II AMI. A type I AMI, also known as a spontaneous MI, refers to a myocardial infarction caused by an atherothrombosis or blood clot forming in the lumen of a coronary artery and causing a sudden (partial or complete) occlusion which significantly decreases the flow of blood through the coronary artery. What precedes the formation of an atherothrombosis is the loss of integrity that occurs at the level of an atherosclerotic plaque's protective covering (fibrous cap) resulting in the release of its thrombogenic and lipid-rich contents into the lumen of a coronary artery following plaque erosion, plaque rupture, fissuring, or dissection (Lilly, 2013). Following the exposure of the plaque's content coming into contact with the blood, the activation of the coagulation cascade, and the formation of an atherothrombosis follows (Burke et al., 2014). Conversely, a type II AMI, also known as secondary MI, refers to a myocardial infarction that is not the result of a primary coronary artery event/atherothrombosis. Examples of the causes that lead to type II AMIs are the following: coronary artery spasm, coronary embolism, anemia, and hypotension (Thygesen et al., 2012).

When diagnosing an acute myocardial infarction, clinicians rely on identifying the following criteria: acute onset of angina (chest pain), symptoms of ischemia along with electrocardiograms showing new ST-elevation, abnormal Q wave, or new left bundle branch block (LBBB), and evidence of myocardial necrosis through the use of blood tests to detect a rise and/or fall of cardiac biomarker values such as cardiac troponin (cTn) and creatine kinase myocardial band (CK-MB) (Thygesen et al., 2012). The reasoning behind utilizing these biomarkers is that once cardiac muscle/myocardium is injured, its cardiomyocytes will release

these biomarkers into the bloodstream at a greater rate. On the other hand, if a cardiac muscle injury has improved, via reperfusion treatments, these cardiac biomarkers would decrease (Antman et al., 1996). As a result, the assessment of cardiac biomarkers like cardiac troponin (cTnI and cTnT) levels in the blood have been implemented and used as a diagnostic indicator of myocardial damage, and thus useful in diagnosing and managing the type of myocardial infarction or other various forms of heart muscle damage presently taking place in a patient(Lilly, 2013). As an added piece of information, the initial rise in troponin levels in the blood occurs within 2-3 hours after an MI and according to a recent finding, levels may persist and be elevated for up to 2 weeks after an MI (Aydin et al., 2019)

Another form of assessing or diagnosing an acute myocardial infarction is through imaging techniques such as transthoracic echocardiography (TTE). As a non-invasive imaging technique, transthoracic echocardiography (TTE) allows one to detect the following: the number of segments displaying regional wall abnormalities during a myocardial infarction, the size of an infarct, the progress of a healing or healed myocardial infarction, as well as adverse ventricular remodeling resulting from a myocardial infarction. (Abouzaki & Abbate, 2016). An additional non-invasive imaging technique is the cardiac magnetic resonance imaging (cMRI or CMR). The application of cMRI with the use of gadolinium enhancement allows clinicians to take more precise measurements and tissue characterization than TTE, such as being capable of distinguishing between reversible and irreversible myocardial injury (Abouzaki & Abbate, 2016) (Fieno et al., 2000). Thus, it is oftentimes labeled as the gold standard in diagnosing and evaluating the progression of an AMI (Bhatt et al., 2017).

After an assessment of the AMI has been made, the main goal of treatment is to salvage ischemic cardiomyocytes of the myocardium thereby limiting the progression of ischemic

necrotic cell death. To accomplish this, focus is placed on timely/prompt reperfusion methods like the following: antithrombotic drugs to dissolve the thrombus (thrombolytics), and percutaneous coronary intervention (PCI) that includes the utilization of emergency catheterization and coronary stents (or drug-eluting stents) to help open or increase the diameter necessary to restore blood flow in plaque-occluded coronary arteries.

All things considered, the combined utilization of electrocardiograms, cardiac biomarker tests, and non-invasive imaging techniques, are vitally essential. Thanks to these medical advancements, clinicians are better able to diagnose AMIs, evaluate infarct size and develop appropriate and timely reperfusion strategies, that are not only vital in salvaging damaged myocardial tissue, but also important in preventing adverse cardiac remodeling and post-MI heart failure, thereby improving survival rates and prognosis of patients who have undergone an AMI (Bhatt et al., 2017)

1.1.3 Adverse Ventricular Remodeling

Following myocardial ischemia and subsequent acute myocardial infarction, treatment in the form of reperfusion and pharmacological medications is time-sensitive and will affect the prognosis of patients undergoing a myocardial infarction. Consequently, patients, who receive reperfusion treatment past optimal/therapeutic treatment times, will be at higher risk of developing larger transmural infarcts, adverse ventricular remodeling, wall rupture, and even heart failure (Abouzaki & Abbate, 2016)

To prevent these detrimental outcomes and to maintain circulatory function, namely stroke volume (SV) and cardiac output (CO), the heart employs an acute compensatory response known as ventricular remodeling (Weisman et al., 1985). According to scientific literature, the

term ventricular remodeling refers to morphologically characteristic changes that include dilation of the ventricle, disproportionate thinning and dilation of the infarcted region, formation of a scar, and geometrical changes in the overall LV shape (i.e. ellipsoid to more spherical shape) (Weisman et al., 1985). These compensatory effects are regulated by the Frank-Starling mechanism, neurohormonal activation (SNS and RAAS), and the body's innate immune inflammatory response.

During the first 3-4 days after an AMI, myocardial cell death, loss of contractility (systolic dysfunction), and area of necrosis progresses in the LV. In response to myocardial cell death, an influx of inflammatory cells removes cellular debris and promotes the destruction of collagen scaffolding that helps maintain ventricular shape. (Cleutjens et al., 1995). Additionally, it is important to note that the degree of this inflammatory response to myocardial injury varies according to the size of the infarct and to each individual's genetic and epigenetic factors that control inflammation (Stylianou, 2019).

Furthermore, ventricular remodeling can occur with the intent of preserving the heart's cardiac output (CO) by way of stretching LV myocardial fibers, resulting in regional thinning and acute dilatation of viable myocardium in the infarcted areas. Consequently, the dilatation of the LV myocardium increases the preload/amount of blood returned to the heart (LVEDV) via the Frank-Starling mechanism. This increase in preload, from LV dilation and stretching of LV myocardial fibers, creates an increased tension between cardiomyocytes' filaments (Mann, 2011), that leads to an increase in the force of contraction (inotropic activity) from ß-adrenergic receptor stimulation, thereby increasing stroke volume and adequately maintaining the heart's cardiac output (Westman et al., 2016a).

Weeks to months following an AMI, progressive ventricular remodeling, LV dilatation coupled with non-compliant scar formation, increases wall stress in the LV chamber, and causes myocardium to undergo eccentric hypertrophy (M. Pfeffer E. Braunwald, 1990). This increase in wall stress, according to the Laplace relationship can lead to further LV dilatation that causes the heart to become less elliptical and more spherical (Westman et al., 2016b)

Other factors that drive adverse cardiac remodeling are neurohormonal activation regulated by the sympathetic nervous system (SNS) and the renin-angiotensin-aldosterone system (RAAS). In response to decreased CO, the SNS releases epinephrine and norepinephrine which affects the heart by increasing, peripheral vascular resistance, HR, SV, BP, and contractility when ß-adrenergic receptors are stimulated. It is particularly useful in helping the body and tissues meet increases in O2 demand whether during exercise or even during an AMI. Conversely, persistent SNS activation by way of catecholamines leads to detrimental effects on the recovering or post-infarcted heart such as hypertrophy, enhanced apoptotic pathways, and reduced cardiac function that all promote fibrosis and further damage (Bhatt et al., 2017)

Chronic SNS activation also promotes the renin-angiotensin-aldosterone system (RAAS) activation. Through the RAAS, the enzyme renin cleaves angiotensinogen to angiotensin I which is then cleaved by angiotensin-converting enzyme (ACE) to help convert angiotensin I to angiotensin II. The increased expression of angiotensin II promotes vasoconstriction and has a direct cytotoxic effect on cardiac myocytes, leading to the acceleration of apoptosis and the promotion of cell hypertrophy. In addition, studies in animal models have shown that angiotensin II infusion leads to increases in perivascular and interstitial collagen content (Sigusch et al., 1996) as well as aldosterone secretion which promotes sodium reabsorption and fluid retention,

9

impairment of arterial compliance, increases in total peripheral resistance (TPR), and HTN (Lilly, 2013).

All things considered, as time passes adverse ventricular remodeling modulated by inflammation, non-compliant scar formation, and neurohormonal activation can lead to further LV dysfunction and reduced cardiac output that can result in volume overload and develop into ischemic heart failure (Lilly, 2013).

1.1.4 Heart Failure

Heart failure (HF) is a disease whose onset can be chronic (compensated heart failure) or acute (decompensated heart failure). As a clinical syndrome, heart failure is often attributed to being a final common pathway of many cardiac diseases resulting in a decrease in cardiac output that causes patients to experience dyspnea, fatigue, poor-exercise intolerance, and volume overload. In addition, heart failure patients can also display orthopnea, paroxysmal nocturnal dyspnea (PND), edema, and abdominal distention (ascites). The manner in which a decreased cardiac output can lead to heart failure symptomatology results from many functional or structural heart disorders that can impair the ventricles' systolic and diastolic function. Some of these disorders, such as coronary artery disease (CAD), hypertension (HTN), dilated cardiomyopathy (DCM), or an AMI, affects the heart's ability to pump blood, to the point of no longer being able to meet the body's metabolic O_2 demand. Along those lines, more than 2/3 of all HF cases can be attributed to 4 underlying conditions: Ischemic heart disease (CAD), chronic obstructive pulmonary disease (COPD), hypertensive heart disease, and rheumatic heart disease. (Hawkins et al., 2009).

There are two types of HF that are categorized based on left ventricular ejection fractions (LVEF). The first type of heart failure, heart failure with reduced EF (HFrEF), is a form of heart failure that is directly caused by systolic dysfunction and the ventricle's diminished capacity to eject blood. The systolic dysfunction that occurs in HFrEF is characterized by a left ventricular ejection fraction $\leq 40\%$ along with concurrent HF symptoms. Furthermore, systolic dysfunction is caused by secondary cardiac issues that alter myocardial cell function, through inflammatory processes, cell death, and fibrosis. As a result, damage caused by MI is commonly associated with HFrEF (Gerber et al., 2016). The second type of HF, heart failure with preserved EF (LVEF $\geq 50\%$), refers to heart failure symptoms caused by diastolic dysfunction resulting from the ventricle's diminished capacity to relax and fill during diastole. Conditions that lead to diastolic dysfunction include cardiac issues that increase the stiffness of the ventricular wall by way of LV hypertrophy, or fibrosis. A common sign displayed by HFpEF patients is vascular congestion due to elevated diastolic pressure in the ventricles being transmitted in a retrograde manner to the pulmonary and systemic veins (Lilly, 2013). As a whole, the distinction between HFrEF and HFpEF and their etiologies continues to be vital in guiding therapeutic interventions for the growing number of HF patients.

According to clinical guidelines, there is no single diagnostic test for HF. Instead, diagnosing heart failure involves a combination of physician assessments, biomarker studies, imaging data from non-invasive techniques (TTE, cMRI), or invasive hemodynamic catheterization (Yancy et al., 2016). After completing these assessments, clinicians are able to evaluate at-risk and current heart failure patients by way of the American College of Cardiology Foundation/American Heart Association and New York Heart Association functional classification systems. The ACCF/AHA stages of HF place emphasis on the development and

progression of disease, whereas the NYHA classes place emphasis on an individual's exercise capacity and their present symptomatic status of the disease (Yancy et al., 2016). By focusing on different aspects of HF, both classification systems are important in helping to provide appropriate guideline-directed medical therapy (GDMT).

Currently, GDMT for heart failure is complex and utilizes an array of therapies that can be pharmacological, interventional, or surgical. The goal of these therapies is to regulate and keep the once compensatory mechanisms in physiological range, manage symptoms, and prevent and limit further decline. However, even with current and improved guideline-directed medical therapies, the absolute mortality rate for patients with HF is approximately 50% within the first five years of diagnosis (Roger et al., 2012). It appears that once a patient reaches HF, what follows is a vicious trajectory of morbidity and mortality that involves multiple hospital readmissions, numerous medications prescribed, and debilitating symptoms that significantly affects the quality of life. For these reasons, medical research continues to strive to find ways to not only improve GDMT but also prevent the development of HF, whether through improvements in diet, activity, and medications.

One way that GDMT seeks to improve upon is in the utilization of pharmacological therapies to target risk factors such as ischemic heart disease and compensatory mechanisms that lead to adverse ventricular remodeling and heart failure. Currently neurohormonal blockade/antagonism is the cornerstone of GDMT for the prevention of adverse ventricular remodeling in patients with MI (Ponikowski et al., 2016). Seeing that compensatory mechanisms are regulated by neurohormonal signaling pathways, many types of neurohormonal antagonist medications have been developed such as ACE inhibitors, angiotensin-receptor blockers (ARB), ß-blockers, and mineralocorticoid-receptor antagonists.

Furthermore, due to preclinical (Toldo et al., 2019) and clinical (B. W. Van Tassell et al., 2017) findings, evidence has been mounting in support of classifying inflammatory responses as a major contributor in the pathophysiology of MI, adverse cardiac remodeling, and HF (Van Linthout & Tschöpe, 2017). As a result, there has been a gradual shift in ideology from targeting solely neurohormonal and atherosclerotic mechanisms, to also targeting and attenuating the inflammatory processes during the stages that lead up to HF as well as after its onset, with the goal of improving symptoms and preventing HF progression.

One particular human clinical trial that has spearheaded the shift in ideology to target and label inflammation as a pathogenic contributor to cardiovascular disease, is the Canakinumab Anti-inflammatory Thrombosis Outcomes Study (CANTOS). In 2011, this large-scale, randomized, double-blind, placebo-controlled clinical trial began. In total it consisted of testing 10,061 patients in 39 countries with previous AMI and high levels of CRP ($\geq$2mg/L), and at median follow-up of 3.7 years to see whether an anti-inflammatory drug, canakinumab -- a monoclonal antibody blocking interleukin-1ß (IL-1ß), could prevent and lower rates of recurrent cardiovascular events. The results, published in 2017, showed that patients taking canakinumab (150 mg/3 months) had reduced CRP levels and significantly reduced cardiovascular events independent of lipid levels, thus providing proof-of-principle that adequate inhibition of the inflammatory pathway from IL-1ß to IL-6 to CRP can significantly reduce cardiovascular events (Ridker et al., 2017) (Abbate, 2017).

1.1.5 Inflammation in AMI

Inflammation is mainly an innate immune response that is highly coordinated. Its purpose is to prevent infection, induce innate and adaptive immune processes, as well as stimulate

healing at the site of injury or infection through leukocyte chemotaxis. With an etiology that can be infectious or non-infectious, inflammation can occur in response to various pathogenic factors like bacteria, viruses, and other microbes, or due to non-infectious triggers and signals resulting from tissue injuries such as trauma, physical injury, toxins, burns, or cell death (that occurs following a myocardial infarction) (Chen et al., 2018). Additionally, there are specific organs that exhibit organ-specific inflammatory responses that are modulated according to an individual's immune capabilities as well as to the site of injury or infection. These organs include the heart, pancreas, liver, kidney, lung, and brain (Chen et al., 2018).

The responsibility of initiating and regulating the acute inflammatory response relies mostly on innate immunological cells such as neutrophils, tissue macrophages derived from circulating monocytes, and dendritic cells. In order to destroy and remove pathogens and cell debris, these innate immunological cells detect molecular signals through the use of germ-line-encoded pattern-recognition receptors (PRRs) (Hirayama et al., 2018). PRRs are capable of detecting/recognizing microbial structures such as pathogen-associated molecular patterns (PAMPs) and damage-associated molecular patterns (DAMPs) that can lead to the formation of cytosolic macromolecular complexes (inflammasomes) and the downstream release of inflammatory mediators (chemokines and cytokines: IL-1ß, IL-6 TNF-α etc.). The release of pro-inflammatory mediators from the cell are what lead to increased vascular permeability resulting in the following: increased recruitment of leukocytes to the site of injury/infection, the release of inflammatory markers/proteins (e.g. CRP, fibrinogen) from the liver, as well as the clinical signs of inflammation – pain, fever, redness, edema/swelling, and loss of function (Chertov et al., 2000)

Pattern-recognition receptors are subdivided into two major classes based on their cellular localization (Bedard et al., 2019). The first major class of PRRs is found in the cell membrane: Toll-like receptors (TLRs) and C-type lectin receptors (CLRs) (Medzhitov, 2010). The second class of PRRs is cytoplasmic PRRs and they include retinoic acid-inducible gene (RIG-I-Like) receptors, the AIM2-like receptors (ALRs), and the NOD-like receptors (NLRs) (Bedard et al., 2019). Among these cytoplasmic PRR sensors NLRs, ALRs and pyrin trigger a distinct defense mechanism that leads to the assembling of cytosolic macromolecular protein complexes, known as inflammasomes, which are responsible for utilizing caspase-1 to process pro-interleukin-1ß (IL-1ß) and pro-IL-18 to their mature forms. Thus, the importance in understanding the functioning/physiological mechanisms of PRRs is indispensable seeing that PRRs and inflammasomes are what allow innate immune cells to initiate acute inflammatory responses thereby acting as the body's first line of defense against PAMPs and DAMPs in the extracellular milieu (Martinon et al., 2002).

Much of what we know from the inflammatory response that follows a myocardial infarction comes from preclinical studies on mice. In Figure 1 we see a descriptive diagram demonstrating the types of inflammation that follows an AMI. Beginning with the inflammatory phase in which an intense sterile inflammation leads to immune cells being recruited to serve in digesting and removing damaged cells ($\approx$0 - 4 d in mice), followed by a reparative and proliferative phase in which neovascularization occurs along with inflammation being suppressed and resolved ($\approx$4 -14 days) (Prabhu et al., 2017).

As important as it is for immune cells to initiate an acute inflammatory response, it is also important for them to have mechanisms in place to resolve inflammation when no longer necessary. A regulated inflammatory response utilizes a combination of the following

mechanisms to terminate an inflammatory response: upregulation of anti-inflammatory cytokines/molecules (such as IL-10), downregulation of pro-inflammatory cytokines, short half-life of inflammatory mediators, and the cessation of tissue infiltration by neutrophils that results in the initiation of programmed cell death (apoptosis) and subsequent neutrophil clearance by phagocytosis from macrophages (Freire & Van Dyke, 2013). Furthermore, an inflammatory response is considered resolved with the departure of macrophages through the lymphatic system (Ortega-Gómez et al., 2013). In addition to the processes that resolve inflammation during the reparative phase, scar formation mediated by fibroblasts and myofibroblasts occurs, due to the heart's limited capacity to regenerate after injury (≈4 -14 days).

However, in the weeks to months that follow an AMI, if post-infarction inflammation is not suppressed and continues, then this form of post-infarction chronic inflammation coupled with overactive fibrosis can lead to additional tissue damage, increasing interleukin-1ß (IL-1ß) release, maladaptive scar formation, and adverse ventricular remodeling. All of which increase the risk of developing HF (Prabhu et al., 2017).

As a result, today inflammation as a pathogenic contributor to disease is a focus of research in many different fields involving diabetes mellitus (Goldfine & Shoelson, 2017), ALS (Meissner et al., 2010), cardiovascular disease (B. W. Van Tassell et al., 2017), and cancer research (Mantovani et al., 2008).
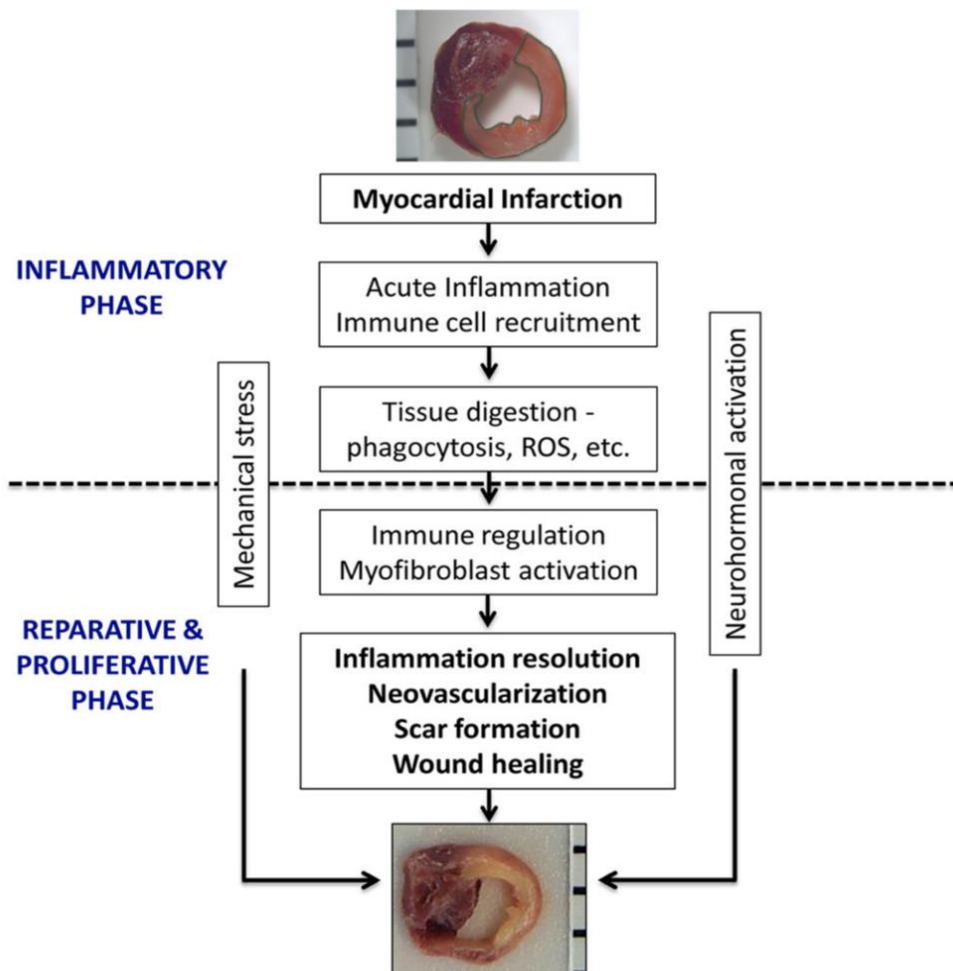
Figure 1: Inflammation post-acute myocardial infarction (Prabhu et al., 2017)

1.2 The NLRP3 Inflammasome

The inflammasome, identified first in 2002 by Dr. Jurg Tschopp and colleagues (Martinon et al., 2002), is a macromolecular protein complex responsible for sensing danger signals, activating caspases, and pyroptotic release of pro-inflammatory cytokines initiating inflammatory signaling pathways (Swanson et al., 2019) (Toldo & Abbate, 2018).

Since Tchopp and colleagues' groundbreaking work, other studies (Martinon et al., 2006) have identified and elucidated the regulatory mechanisms, oligomerization components, and

agonists of different types of inflammasomes named after the pattern-recognition receptor (PRR) regulating their activity (Lamkanfi & Dixit, 2014). Some of these inflammasomes include the NRLP1, NLRP3, NLRC4, and AIM2 inflammasomes. More importantly these findings from these initial studies have helped in detailing the role and delicate balance that inflammasomes help maintain during an innate immune inflammatory response. In particular when physiologically regulated, inflammasomes play an integral role in controlling innate immune pathways responsible for inflammation, host defense, and protection from injury and sepsis (Dagenais et al., 2012). Conversely, inflammasomes that are over-stimulated or not sufficiently suppressed can lead to exuberant inflammatory responses that are linked to many different inflammatory diseases (Dagenais et al., 2012).

Of all the inflammasomes that have been identified, the NLRP3 inflammasome is the one that has been most characterized (Toldo & Abbate, 2018). Similar to other inflammasomes, the NLRP3 inflammasome can aptly be described as a finely regulated macromolecular protein complex that activates a caspase -- caspase-1, and processes and releases pro-inflammatory cytokines such as IL-1ß and IL-18. Furthermore, what makes the NLRP3 inflammasome an important topic of research is the pathophysiological role it plays in acute to chronic inflammatory responses that contribute to many different inflammatory diseases, as well as its ability for sensing a wide variety of both intracellular danger and extracellular alarmin signals (Franchi et al., 2012). The following includes a list of common PAMPs and DAMPs (NLRP3 agonists/stimuli):

- **DAMPs** = MSU (monosodium urate) crystals, Ca^{++} influx, mROS (mitochondrial reactive oxidative species), extracellular ATP (eATP), uric acid, cholesterol,

hydroxyapatite crystal, silica, aluminum salts, asbestos, and fatty acids
(Franchi et al., 2012)

- **PAMPs** = pathogens that include viruses (influenza A), bacteria (LPS, Neisseria gonorrhoeae), gram-negative bacteria, and bacterial toxins like nigericin and maitotoxin. Broz and Dixit have suggested that low intracellular potassium concentrations that occurs from potassium release (K^+ efflux) is associated with all NLRP3 activators, and thus may one day be proved to be sufficient enough on its own to trigger NLRP3 activation (Broz & Dixit, 2016) (Muñoz-Planillo et al., 2013).

Additionally, these DAMPs/PAMPs are responsible for binding to and activating membrane-bound Toll-like receptors (TLRs). Once TLRs in the membrane are activated the resulting signal produced by DAMPs or PAMPs are transmitted into the cell and towards the nucleus as a downstream signal that is mediated by myeloid differentiation factor-88 (MyD88) and interleukin-1 receptor-associated kinase -1, -4 (IRAK1/4) which will activate NF-κB activity resulting in gene expression of the NLRP3 inflammasome components and proteins (Dagenais et al., 2012).
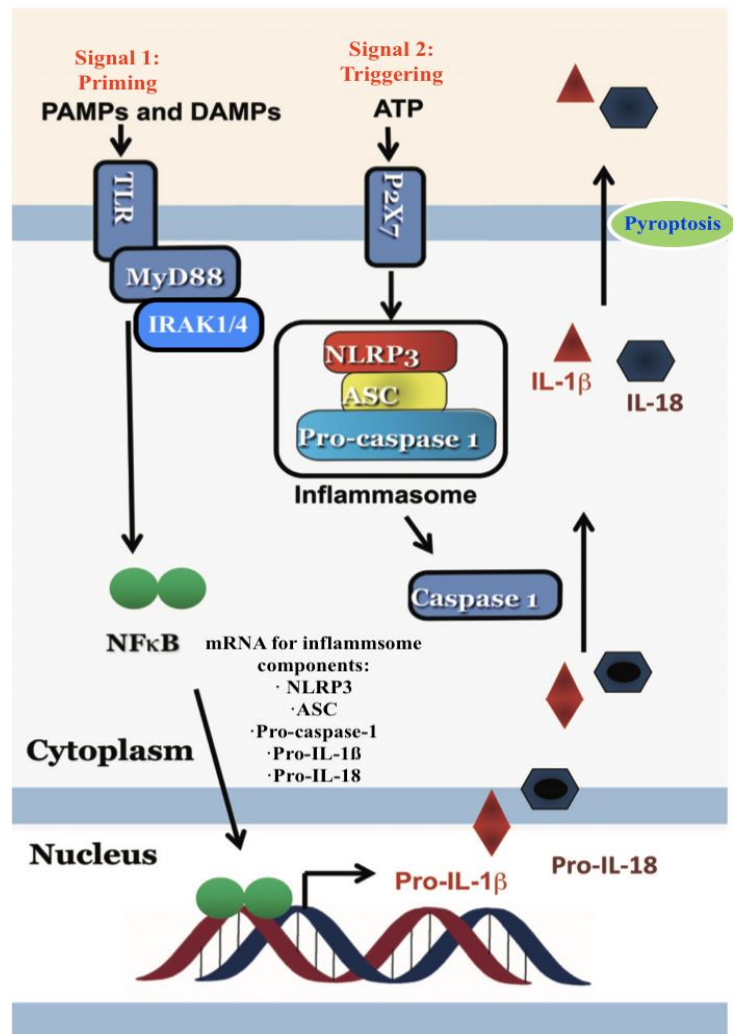
Figure 2: NLRP3 priming step (signal 1) and triggering step (signal 2) (O'brien et al., 2014)

19

The three NLRP3 (cryopyrin) inflammasome components produced are a sensor protein (NOD-like receptor), adaptor protein (ASC), and an effector protein (caspase-1), which come together by way of homotypic pyrin domain (PYD-PYD) and caspase recruitment domain (CARD-CARD) interactions (Lu et al., 2014). Before detailing the two-step process of activating and forming the NLRP3 inflammasome below is a brief summary detailing the components and proteins involved in regulating its formation.

The first component of the NLRP3 inflammasome serves as the sensing component which consists of NLRP3 itself. NLRP3 contains a leucine-rich repeat domain at the C-terminal, an NLR/NBD/NACHT domain at its center, and a pyrin domain at the N-terminal responsible for binding to the second component of this inflammasome (Martinon et al., 2006).

The second NLRP3 inflammasome component is the apoptosis speck-like protein containing a CARD (ASC) which serves as the adaptor protein. The adaptor protein ASC consists of a pyrin domain (PYD) and a caspase activation and recruitment domain (CARD). The function of ASC is to help recruit procaspase-1 for the purpose of associating ASC and procaspase-1 with NLRP3, thus bridging the sensor component (NLRs) with the downstream adaptor and effector (caspase-1) (Martinon et al., 2006).
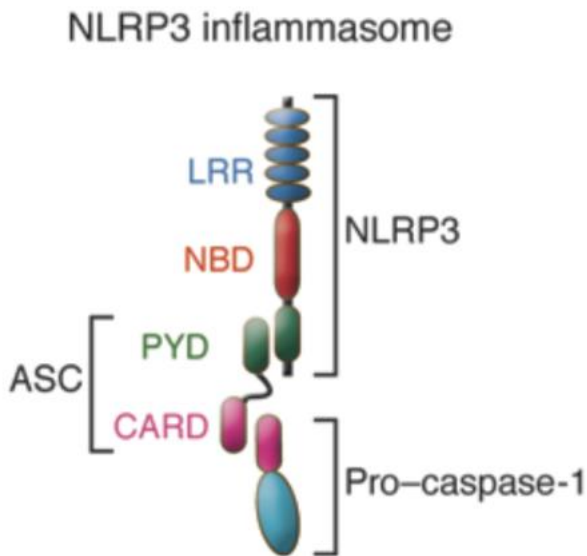
Figure 3: The NLRP3 components

The third component, caspase-1, is a cysteinyl aspartate-specific protease. Caspase-1 is initially produced as an inactive precursor pro-caspase-1. Pro-caspase-1 consists of a CARD, p20, and p10 subunits. After pro-caspase-1 is proteolytically cleaved, two p20 and two p10 subunits will assemble into the active caspase-1, a heterotetramer that is responsible for cleaving pro-IL-1ß and pro-IL-18 to IL-1ß and IL-18 respectively and inducing pyroptosis, a cell death process that will be further described in a later section (Broz et al., 2010)

In addition to the three main components that form the NLRP3 inflammasome, there are other proteins such as Nek7, MARK4, and MAVs that have recently been investigated and suggested to regulate NLRP3 inflammasome formation and activation.

Nek7 is a serine-threonine kinase and member of the family of mammalian NIMA-related kinases (Neks) (De Souza et al., 2015) (He et al., 2016). According to research findings, Nek7 contributes to mitotic spindle assembly during early mitosis by localizing to the centrosome to ensure mitotic progression (De Souza et al., 2015) (Schmid-Burgk et al., 2016). In addition, Nek7 is an NLRP3-binding protein that acts downstream of potassium efflux and is presumed to regulate the assembly and activation of the NLRP3 inflammasome (Schmid-Burgk et al., 2016). A study in 2016 showed that when Nek7 is absent, NLRP3 inflammasome response is blunted as evidenced by lower levels of caspase-1 and IL-1ß release. This study also showed that Nek7 only affects the NLRP3 inflammasome, thus displaying specificity in that no other inflammasomes (i.e. NLRC4 nor AIM2) showed marked effects by Nek7 binding (Schmid-Burgk et al., 2016)

Microtubule-affinity regulating kinase 4 (MARK4) is an evolutionarily conserved protein whose function is to regulate microtubule dynamics through phosphorylating microtubule associated proteins (MAP) (Trinczek et al., 2004). Additionally, Li et al. have shown that MARK4 are important in regulating NLRP3 inflammasome sorting and activation. The manner

21

MARK4 regulates NLRP3 inflammasome activation is suggested to be by binding to NLRP3 and driving it to the microtubule-organizing center (MTOC), the site of NLRP3 inflammasome activation, via microtubule-based transport (Li et al., 2017).

Mitochondrial anti-viral signaling proteins (MAVS) is another protein that is presumed to associate with the NLRP3 inflammasomes and facilitate its oligomerization. A 2013 study showed that when knocking down MAVS expression in THP-1 and mouse macrophages, there was an attenuation of NLRP3 inflammasome activation. Furthermore, the study ultimately suggest that MAVS facilitates the recruitment of NLRP3 to the mitochondria and may enhance its oligomerization and activation by bringing it in close proximity to mROS (Park et al., 2013; Subramanian et al., 2013)

1.2.1 NLRP3 Inflammasome Formation Pathway

The activation and formation of the NLRP3 inflammasome require two independent steps that are labeled as the priming and triggering steps. The main objective of the priming step is to induce the expression of NLPR3 inflammasome components via signaling pathways from the TLRs on the cell membrane and NF-κB activation, thereby priming the cells to respond in the event of injury or pathogen exposure. Therefore, when extracellular primary signals, created by cellular debris or microbial products (DAMPs/PAMPs), bind to and stimulate Toll-like receptors (TLRs) located on the cell membrane, downstream signaling will activate the NF-κB activity. NF-κB (nuclear factor kappa-light-chain-enhancer of activated B cells) is a protein complex located in the cytoplasm that is capable of controlling cytokine production, and DNA transcription (i.e. gene expression) resulting in the translation and production of inflammasome components and cytokines such as NLRP3, ASC, pro-caspase-1, pro-IL-1ß, and pro-IL-18.

Furthermore, as mentioned previously the downstream signaling that activates NF-κB activity in the nucleus is mediated by MyD88 and IRAKs. Despite primary signals activating gene expression and formation of the individual NLRP3 components during the priming step, NLRP3 inflammasome activation, oligomerization, and IL-1ß processing do not occur without a trigger/distress signal (Kelley et al., 2019).

According to experimental studies, one example of a trigger/distress signal capable of activating the NLRP3 inflammasome has been the production of mitochondrial reactive oxygen species (mROS) resulting from mitochondrial damage and oxidative stress (Muñoz-Planillo et al., 2013) (Dagenais et al., 2012). It has been suggested that mROS production not only induces NF-κB-dependent gene expression seen in the priming step, but also NLRP3 inflammasome oligomerization that prepares the cell for inflammasome activation (Dagenais et al., 2012)

Another example of distress signals capable of activating the NLRP3 inflammasome is K+ efflux and cathepsin B release resulting from lysosomal destabilization. K+ efflux can also result from an increase in cell death that causes extracellular ATP (eATP), a byproduct of cell death, to attach to cells with P2X purinoreceptor 7 (P2X7) and induce inflammasome formation (Mezzaroma et al., 2011) (Franchi et al., 2012). Following the increase in K+ efflux and the resulting lowered K+ intracellular concentration, a cytosolic serine/threonine-protein kinase (Nek7) senses K+ efflux and subsequently regulates the oligomerization and recruitment of NLRP3 components (Schmid-Burgk et al., 2016).

Once the NLRP3 oligomerization process is induced, a circular structure is formed with a central core that becomes the site of ASC polymerization. Originating from this central core of polymerized ASC, a large number of pro-caspase-1 enzymes will be recruited, cleaved, and activated into caspase-1 filaments that form a star-like structure that consists of numerous

caspase-1 enzymes capable of enzymatically cleaving inactive pro-inflammatory cytokines pro-IL-1ß and pro-IL-18 into active pro-inflammatory cytokines IL-1ß and IL-18 respectively. In addition, activated caspase-1 cleaves gasdermin D (GSDMD) which induces pyroptosis, a programmed cell death responsible for pore formation and the release of pro-inflammatory cytokines and intracellular/cytoplasmic content that further induces pro-inflammatory responses (Swanson et al., 2019) (Takahashi, 2019).
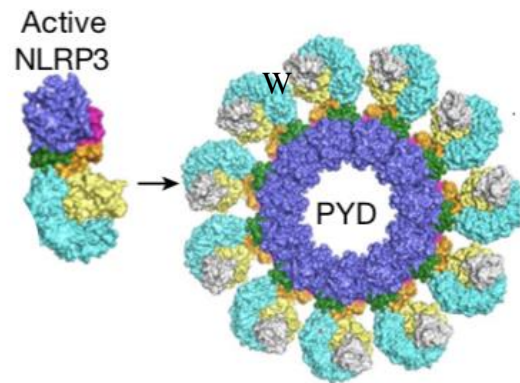
Figure 4: Structure of the NLRP3 oligomer

1.2.2 IL-1 Family Pro-inflammatory Cytokines Release Processes

Cytokines make up a large group of proteins that are released by cells of the immune system. Some examples of cytokines include chemokines, interferons, TNFs, and interleukins (ILs). The function and release of cytokines are important in mediating the signaling pathways involved in immunity and inflammation. To induce their effects on signaling pathways, cytokines can be released by a general conventional model, or a non-conventional model.

Through the general conventional model, which describes how most cytokines are secreted out of the cell, cytokines are first encoded and synthesized by genes that are inducible by inflammatory transcription factors (TFs) like NF-κB, and AP-1 (Smale & Natoli, 2014). Once synthesized, cytokines that contain N-terminal secretion sequences will be able to insert into the

endoplasmic reticulum (ER) in a co-translational manner (Lieberman et al., 2019). From the ER, cytokines will eventually be released into the extracellular space where they then bind to their appropriate receptors and promote inflammatory responses (Lieberman et al., 2019).

The other form of extracellular cytokine release, releases the most potent molecules of the innate immune system, the IL-1 family cytokines(i.e. IL-1α, IL-1ß, IL-18, and 8 other cytokines), through a process mediated by Gasdermin D (GSDMD), a pore-forming protein that consists of a C-terminus that auto-inhibits the pore-forming activity of its N-terminus (Kayagaki et al., 2015). Perhaps the most important cytokine released by this form of cytokine release is IL-1ß, a pro-inflammatory cytokine that is initially formed as an inactive precursor. When activated IL-1ß functions not only as a potent pyrogen (a substance that produces fever) but also as an important signal that induces the synthesis and expression of several hundred downstream/ secondary inflammatory mediators (Dinarello, 2011). To induce these effects extracellular signals must first activate the NLRP3 inflammasome leading to autocatalytic activation of its effector -- caspase-1. Upon activation, caspase-1 proteolytically cleaves pro-IL-1ß, pro-IL-18, and Gasdermin D resulting in mature IL-1ß and IL-18 as well as Gasdermin-D's N-terminal fragment that is now capable of forming pores within the cell membrane (Liu et al., 2016). In addition, caspase-1 is also known to cleave several proteins from the Krebs cycle which triggers a dramatic decrease in cell energy production resulting in cell swelling and rupture (Shao et al., 2007). Consequently, the loss of cell membrane integrity resulting from the formation of a pore by GSDMD, cell swelling, and rupture of the membrane allows for the release of intracellular contents and pro-inflammatory cytokines into the extracellular space, a cell death process also known as inflammasome-mediated pyroptosis (Lamkanfi & Dixit, 2014; Shi et al., 2015).

1.3 The Role of the NLRP3 Inflammasome following Myocardial Injury

The role of cardiac inflammation, following myocardial injury, is to restore homeostasis by eliminating and removing offending agents (cell debris and dead cells/tissue) from the area of injury, which helps to bring about healing and wound repair by way of scar formation to the injured myocardium. However, several reports have now demonstrated that excessive inflammation modulated by the NLRP3 inflammasome, and IL-1ß processing has a role in pathophysiological processes that contribute to AMIs, cardiac remodeling, and compensatory mechanisms leading up to HF (Kawaguchi et al., 2011; Mezzaroma et al., 2011; B. W. Van Tassell, Toldo, et al., 2013).

Beginning with the response to necrotic and apoptotic cell death that occurs during an acute myocardial infarction; studies show that the innate immune system utilizes inflammatory inducers (DAMPs released from necrotic cells: eATP, K+ efflux etc.), membrane sensors (PRRs: TLRs), cytosolic sensors (NLRP3 inflammasomes), and cytokine release (IL-1ß, IL-6, IL-18) to initiate enhanced inflammatory responses (Land, 2015). Responses, that cause local surges of pro-inflammatory cytokines to significantly amplify/exacerbate sterile inflammatory responses by inducing chemotactic recruitment of immune cells (neutrophils, macrophages, and fibroblasts) to the infarcted myocardium, and activating the NLRP3 inflammasomes in leukocytes and cardiac resident cells. Consequently, an enhanced inflammatory response, modulated by NLRP3 inflammasome, leads to increased inflammatory cell death (pyroptosis), additional loss of functional myocardium, further dysregulation in recovery processes (fibrotic non-functional scar formation) and systolic dysfunction that can persist and lead to systemic inflammation seen AMI, adverse ventricular remodeling, and HF (Toldo et al., 2018).

The potential of limiting/attenuating the inflammatory response to help in cardiovascular diseases has led to early experimental studies investigating broad anti-inflammatory interventions using glucocorticoids (Metz et al., 1986) and NSAIDS (Kalkman et al., 1995) and later targeted anti-inflammatory interventions that targeted cytokines, CRP, and NLRP3, some of which are discussed and referenced in a later section. Thanks to what was learned from these studies, many current studies have developed new pharmacological drugs to target the NLRP3 inflammasome and its end products (IL-1ß and IL-18) with the goal of determining the efficacy that targeted anti-inflammatory interventions could have on decreasing cell death, limiting LV enlargement after an AMI, and overall reducing the risk/incidence of heart failure (Mezzaroma et al., 2011) (B. W. Van Tassell et al., 2017)

1.4 Goal of the Study

When applied in a timely manner, reperfusion strategies in the form of percutaneous coronary interventions (PCI), anti-thrombolytic medications, and implantation of stents, have drastically improved survival rates and overall prognosis of AMI patients. However, there are still a number of patients that do not receive reperfusion treatment during the appropriate therapeutic window of time, as well as patients with comorbidities such as diabetes, obesity, advanced age, hypertension, and large infarct sizes, that overall impair the efficacy of GDMT and significantly increases the risk of developing further myocardial injury, adverse ventricular remodeling, and heart failure.

In order to address these concerns, multiple experimental studies along with this present study are investigating the efficacy of utilizing pharmacological strategies to mitigate NLRP3-

modulated inflammatory signals that promote further myocardial injury in cardiovascular diseases.

In contrast to studies investigating the anti-inflammatory effects of targeting downstream NLRP3 mediators of inflammation (IL-1 receptors, IL-1ß, IL-6), this present study was designed to utilize OLT1177 (dapansutrile), a recently developed NLRP3 inhibitor, to target and inhibit the upstream NLRP3 formation process thereby resulting in less caspase-1 being activated, less IL-1ß produced, and overall a decreased sterile inflammatory response. Furthermore, evidence-based research from a previous study suggests that OLT1177, when given promptly to mice following ischemia-reperfusion injury from a transiently ligated AMI, was capable of reducing infarct size and caspase-1 activity, as well as preserving cardiac systolic function thus confirming the potential clinical translational value of utilizing OLT1177 as a cardioprotective strategy after myocardial injury (Toldo et al., 2019). Additionally, previous studies have shown that chronic IL-1ß activity promotes adverse cardiac remodeling, and that IL-1ß inhibition given in the chronic phase of post-AMI remodeling, improves ventricular remodeling and ß-adrenergic responsiveness as well as reduces ventricular filling pressures (Mezzaroma et al., 2011)

Hence, we hypothesize that by administering OLT1177 to inhibit the NLRP3 inflammasome after a myocardial injury we will not only prevent the NLRP3 inflammasome from promoting aberrant inflammasome signaling production, but also mitigate the inflammatory response, thereby improving cardiac remodeling and limiting heart failure. To evaluate this hypothesis, we examined the effects of OLT1177 throughout a 10-week time period in mice following a large nonreperfused AMI and our specific aims for this study included:

1. Measuring the physiological benefit that OLT1177 has on ejection fraction, and

cardiac remodeling through the use of transthoracic echocardiography (TTE)

evaluation.

2. Measuring the effects of OLT1177 on preserving the heart's contractile reserve and ß-

adrenergic responsiveness through the use of isoproterenol challenge and TTE

evaluation.

3. Assessing the physiological benefits that OLT1177 has on limiting systolic and

diastolic dysfunction through the use of LV catheterization (measuring LVEDP, +dP/dT,

-dP/dT, and peak systolic pressure).

Currently, there are no selective NLRP3 inhibitors that are clinically available at this time, thus it

is our aim that the knowledge gained from this research will bring us one step closer to finding

safe and effective ways to use a novel therapeutic class of NLRP3 inflammasome inhibitors to

slow adverse LV remodeling and improve clinical outcomes.

1.5 OLT1177 Therapy

OLT1177 (dapansutrile) is a ß-sulfonyl

nitrile molecule designed to inhibit the NLRP3

inflammasome's capability of producing IL-1ß and
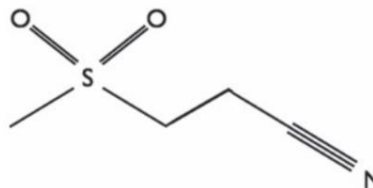
Figure 5: OLT1177 structure

IL-18 inflammatory cytokines. A previous study by Marchetti and colleagues described the

specificity of OLT1177, by demonstrating that it had no effect on other inflammasome types

such as AIM2 nor NLRC4 inflammasomes (Marchetti, Swartzwelter, Gamboni, et al., 2018b).

Additional findings from this study have shown that OLT1177 is safe in humans, therefore its

unique inhibitory effect on the NLRP3 inflammasome has been a topic of research since its

development in 2017 due to its potential for treatment of IL-1ß- and IL-18-mediated diseases.

1.5.1 Routes of Administration

OLT1177's routes of administration used in previous and current studies include the

following: oral route (enriched diet and capsule form), injection route (intraperitoneal), and oral

gavage. For oral OLT1177 administration, OLT1177-enriched diet (3.75g OLT1177 per kg of

food or 4.5g OLT1177 per kg of food) has been used in previous murine studies (Marchetti,

Swartzwelter, Gamboni, et al., 2018a; Toldo et al., 2019) while oral OTL1177 capsules used in

phase I-II clinical trials are currently being investigated in human heart failure patients (clinical

trial identifier: NCT03534297)

In regards to the injection route of administration, OLT1177 injections into the peritoneal

cavity (i.p. injections), have been primarily used in murine studies by first solubilizing crystalline

OLT1177 with sterile saline and subsequently injecting OLT117 using the following doses in

mice: 6, 60, 100 or 600 mg/kg OLT1177 i.p. dose (Toldo et al., 2019), or 200mg/kg OLT1177

i.p. (Sánchez-Fernández et al., 2019). Similarly, oral gavage of OLT1177 involves solubilizing a

dosage of OLT1177 (60, 600mg/kg) but instead of using saline, it is solubilized with distilled

water and subsequently administered to mice (Marchetti, Swartzwelter, Koenders, et al., 2018).

1.5.2 OLT1177 Effects and Mechanism of Action

Much of what is known regarding the effects and mechanism of action of OLT1177

comes from a 2017 report by Marchetti et al. In this report Marchetti and colleagues describe

their results from a phase 1 clinical trial that involved 35 healthy human subjects. Overall, the results from this clinical trial and pharmacokinetic studies demonstrated that OLT1177 at different dosages (100, 300, and 1000mg capsules): has a long half-life (approx. 23 hrs.), is safe (showing no organ toxicities) and well tolerated. This report also contained the results from in vitro, in vivo, and whole cell-patch clamp studies.

From in vitro studies on human blood-derived macrophages (MBDM), murine macrophage cell line, and freshly isolated human blood neutrophils, results demonstrated that OLT1177: specifically targets the NLRP3 inflammasome, prevents NLRP3 inflammasome formation by inhibiting ATPase activity, suppresses caspase-1 activity and IL-1ß and IL-18 release, and has no effect on TNFα and on the priming step of NLRP3 formation. Furthermore, evidence that OLT1177 prevents NLRP3 inflammasome formation was provided through the use of immunoprecipitation and FRET analysis on J774A.1 cells. The results from this experiment demonstrated that OLT1177 prevents NLRP3 oligomerization and activation by directly inhibiting NLRP3 inflammasome's ATPase activity necessary for the recruitment and association of NLRP3-ASC and NLRP3-caspase-1 (Duncan et al., 2007). Without these domain associations, NLRP3 oligomerization is inhibited leading to a reduction in caspase-1 activity, the release of mature inflammatory cytokines (IL-1ß and IL-18), as well as in pyroptotic cell death.

The results from in vivo studies on mice that had undergone LPS-induced systemic inflammation, demonstrated that OLT1177 reduces the severity of systemic inflammation as evidenced by decreased levels of chemokines and cytokines in lung, liver, spleen, and skeletal muscle tissues. In addition, results from in vivo studies demonstrated that OLT1177 increases oxidative metabolism. By way of examining excised muscle tissue, OLT-treated mice displayed an increased reduced glutathione (GSH) and oxidized glutathione (GSSG) ratio, indicating an

improved glutathione homeostasis that is important in antioxidant effects and in oxidative metabolism.

Lastly, the report described utilizing whole-cell patch-clamp technique on human-LPS primed monocytic U937 cells treated with OLT1177 and found that OLT1177 does not inhibit the K^+ ion current change (K^+ efflux), a common activator of the NLRP3 inflammasome. As mentioned earlier, activation of P2X7 receptor by eATP (a byproduct of cell death) results in K^+ efflux from the cell as well as an expected current change to identify while utilizing the whole-cell patch-clamp technique. Consequently, the results from the patch-clamp study led the investigators to conclude that OLT1177 must inhibit the NLRP3 inflammasome by a mechanism downstream of P2X7 receptor activation.

CHAPTER 2: Methods and Materials

2.1 Ethical Approval

All experimental procedures in this study were performed in accordance with the "Guide for the Care and Use of Laboratory Animals" published by the National Institutes of Health (8th ed. revised 2011). The study protocol was approved by the Virginia Commonwealth University Institutional Animal Care and Use Committee.

2.2 Study Design

The main variables that this study tested for in mice with a nonreperfused AMI, are the changes in a 10-week time period that occur to cardiac function (systolic and diastolic function) LV cardiac remodeling, and contractile reserve.

In this present study 60 adult male Imprinting Control Region (ICR) mice (8 weeks old) of 35-45g of weight, supplied by Envigo (Indianapolis, IN) underwent an open-heart surgical procedure. Of these, 54 mice underwent an experimental AMI via permanent ligation of the left coronary artery near its origin (proximal), while the remaining 6 mice underwent a sham operation procedure. Three days after inducing the experimental AMI or sham procedure, the infarct size and cardiac remodeling of the surviving mice (n=35, 58%) were assessed non-invasively via transthoracic echocardiogram (TTE). Based on these echocardiogram values, mice were assigned, utilizing this study's inclusion criteria and comparative analysis, into 1 of 4 groups each with 1 of 3 different diets to eat from for 10 weeks. These 3 different diets were low-dose OLT1177 diet (Group 1), high-dose OLT1177 diet (Group 2), and standard diet

(Groups 3 and 4). Furthermore, all three diets were provided by Research Diets, Inc (New Brunswick, NJ) and administered to mice 1 week after experimental AMI surgery, and repeatedly added throughout the duration of this 10-week study.

At 4-weeks and 10-weeks, all surviving mice (n=28, 47%) underwent a transthoracic echocardiogram along with an isoproterenol challenge to test the heart's contractile reserve. At the end of 10 weeks, 2 of 10 mice (20%) mice had died in the OLT 3.75 gr/kg group, as compared with 2 of 9 mice (22%) in the OLT 7.5 gr/kg group, 3 of 10 mice (30%) in the standard diet group, and 0 of 6 (0%) in the sham-operated group.

Lastly, the mice underwent an invasive LV catheterization procedure and then euthanized by pentobarbital overdose. The hearts were then explanted, along with plasma and stored in a freezer (-80C) for future ELISA analysis.

2.2.1 Experimental AMI Model Procedure

The experimental AMI model used in this study was performed under sterile conditions and involved permanently ligating the left anterior descending coronary artery near its origin. For the purpose of our study, this nonreperfused AMI model was utilized to simulate the drastic changes that occur following a myocardial injury such as adverse cardiac remodeling in the form of ischemic dilated cardiomyopathy and LV hypertrophy. To accomplish this complex, invasive, and high-risk surgery, a skilled investigator performed these surgical procedures utilizing the following protocol.

Each mouse was anesthetized intraperitoneally with the injection of sodium pentobarbital (50-70mg/kg) and subsequently shaved in the left chest area. Next, the mouse was placed and secured in a supine position, intubated, and placed in the right lateral decubitus position. The

mice were connected to a positive-pressure ventilator. The tidal volume of this ventilator was set at 0.25ml, and the respiratory rate was adjusted to 133cycles/min. A left thoracotomy (a surgical procedure allowing access to the thoracic organs: heart and lungs) was performed in the 4th intercostal space. The right lateral decubitus position also allowed access for a pericardiectomy (surgical removal of part or most of the pericardium). Once the heart was exposed, the left anterior descending coronary artery was identified and permanently occluded with the use of a 7-0 silk suture tied around the coronary artery. After each coronary artery occlusion, the thoracic cavity was closed with sutures and the mice were extubated. The mice were then left to recover on heating pads and slow-release buprenorphine (1mg/kg) was administered. Once recovered, the mice were housed under climate-controlled conditions at a 12-hr light/dark cycle and provided with standard mice chow/food and water for the next 7 days, wherein afterward their diet was changed to either standard diet or diet containing low- or high-dose OLT1177. Furthermore, the mice that survived the experimental AMI procedure showed exceptional resilience in the form of eating, drinking, and moving around in their cages normally, and without much discomfort.

In total 54 mice underwent the experimental permanent ligation AMI, while the remaining 6 mice underwent a sham operation procedure that included every step in the protocol except the left coronary artery ligation. A summary of the mortality rate in mice after the AMI procedure (post-operative period) is seen in the following table:

Table 1: The mortality, survival, and incidence of infarction before setting up experimental groups
Attempted open heart surgeries...60
Survival of open-heart surgery + 3d ECHO..................................35 of 60 (58%)
Attempted AMI permanent occlusions..54 of 60 (90%)
Initial Incidence of infarction (successful occlusions)................... 29 of 54 (54%)
Unsuccessful occlusion (i.e. LMI)..1 of 54 (0.02%)
Operative deaths (during AMI or ECHO).....................................11 of 60 (18%)
Late deaths (~1-3d after ECHO)...13 of 60 (22%)

Note: the mice that died in the post-operative period or had unsuccessful occlusions were excluded from the remainder of the experimental results, analyses, and tables.

2.2.2 Test Subject and Inclusion Criteria

Three days (72 hrs.) after AMI surgery, the surviving mice (n=35, 58%) underwent transthoracic echocardiography (TTE). In our present study, TTE was performed three times throughout 10 weeks to assess cardiac function, infarct size, and cardiac remodeling in a non-invasive manner. The results from the initial TTE were particularly important in allowing us to assess and determine which mice would be part of the study and also set up different groups based on our inclusion criteria and exclusion criteria.

The inclusion criteria of this study consisted of the following: mice with a large nonreperfused anterior infarct ($\geq$ 4 akinetic segments involving the anterior wall), an enlarged ventricle (left ventricular end-diastolic diameter [LVEDD] $\geq$ 4.4mm), and systolic dysfunction (left ventricular ejection fraction [LVEF] $\leq$ 40%). Our exclusion criteria consisted of mice that

did not meet the inclusion criteria such as mice with a lateral myocardial infarction (LMI), mice that underwent a sham operation, and mice that did not survive the AMI procedure.

2.2.3 Selection of Control and Experimental groups

After the assessment of the initial 3-day ECHO values, these mice were assigned to four different groups by an investigator not involved in the assessment of endpoints. Below is a description of the four groups and the number of mice that survived the full 10 weeks. Note: these are the mice whose ECHO and LV catheterization values were utilized for this study's results, tables, and figures.

At the end of 10 weeks, all sham-operated mice (n=6), and 41% of the mice (n=22) that had undergone the experimental AMI were alive. Whereas 59% of the mice (n=32) that underwent the experimental AMI had died: during the initial AMI procedure (n=11), shortly after echocardiogram(s) (n= 13), or throughout the 10 weeks due to causes linked to the change in diet (from regular chow to the experimental OLT diet) (n=1), or not surviving anesthesia during week-4 and week-10 echocardiogram assessments (n=4). Furthermore, two of the mice were euthanized due to succumbing to fighting wounds (n=1), or illness (n=1), and one mouse (n=1) was excluded for having an LMI.

- Group 1 consisted of 10 mice that underwent an AMI procedure. The diet that these mice received for 10 weeks was a diet containing OLT1177 (3.75 gr/kg). This diet was also referred to as the low-dose OLT diet and was gray in color.

- Group 2 consisted of 9 mice that underwent an AMI procedure. The diet that these mice received for 10 weeks was a diet containing OLT1177 (7.50 gr/kg). This diet was also referred to as the high-dose OLT diet and was yellow in color.

- Group 3 consisted of 10 mice that underwent an AMI procedure. The diet that these mice received for 10 weeks was the control/standard diet. This diet contained no OLT1177 and was green in color.

- Group 4 consisted of 6 mice that underwent a sham operation. The diet that these mice received for 10 weeks was the control/standard diet. This diet contained no OLT1177 and was green in color.

2.2.4 Treatment with OLT1177 Diet

The experimental treatment tested in this study was OLT1177, a pharmacological NLRP3 inflammasome inhibitor, that was supplemented/admixed into mice chow (0.5" pellets) and color-coded by Research Diets, Inc (New Brunswick, NJ). This diet, which was supplemented with either low- or high-dose OLT1177 (3.75g or 7.50g of OLT1177 per kg of food), was administered 1-week post-AMI to experimental Groups 1 and 2 respectively. Research Diets, Inc (New Brunswick, NJ) also provided the control diet which was labeled as standard/control diet. This control diet did not contain OLT1177 and was administered to Group 3 (control group mice) and Group 4 (sham-operated mice)

Throughout the remainder of this 10-week study, the survival of the animals and the average food consumption of every cage was assessed and recorded every ~1-3 days. To ensure the mice were eating sufficiently, food was added regularly, and further monitoring was done by weighing and recording the weight of each mouse once a week for 10 weeks. In addition, all cages were examined daily, and changed once a week by employees of the Department of Animal Resources.
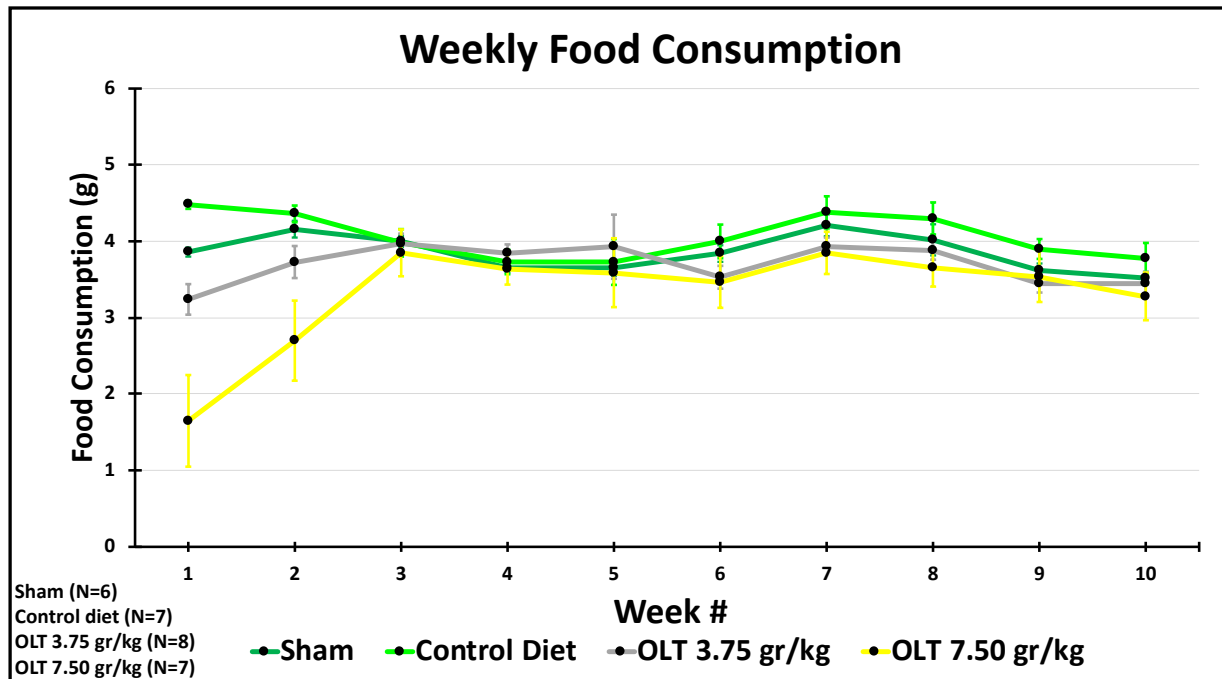
Figure 6: Average weekly food consumption of all four groups during the 10-week study
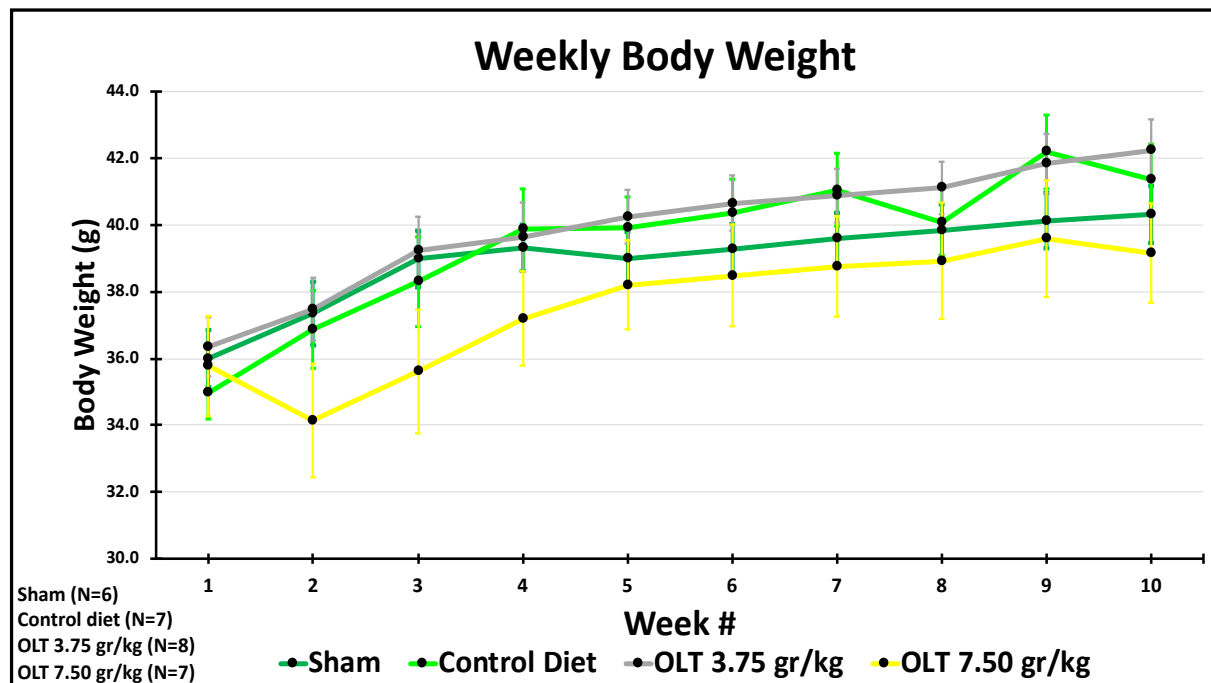
Figure 7: Average body weight of all four groups recorded each week during the 10-week study

As can be seen in Figures 6 and 7, during the first 2-3 weeks of the study, both OLT-treated mice groups consumed considerably lower amounts of their diet, especially the high-dose OLT-treated group. Consequently, the high-dose OLT-treated group (Group 2) also had lower weights than other mice groups. One possible reason for this difference in food consumption and body weight can be due to a period of acclimation to a new diet, with preferences of flavors playing a possible role. Nevertheless, food consumption and body weight of Group 2 mice gradually increased to comparable levels of the other mice groups in the study.

2.3 Transthoracic Echocardiography (TTE)

Transthoracic echocardiography is a noninvasive imaging technique that allows one to monitor and visualize in real-time the heart's morphology, infarct size, and function. To produce images, echocardiography utilizes a piezoelectric crystal contained within a transducer to emit a controlled high-frequency sound (ultrasound) waves that have the capability to travel through any medium (Mohamed et al., 2010). This transducer is also responsible for detecting ultrasound waves/echoes that are reflected back to the transducer from body tissues and converted into electrical signals and images appearing on the echocardiography system screen. These echo signals that are reflected from different body tissues differ in brightness depending on the density of that particular body tissue. For example, dense tissues like pericardium will appear white/bright, whereas hollow tissues like blood-filled chambers of the heart will appear black, signifying that no echo signals were produced/reflected.

In this present study we utilized echocardiography to assess and monitor the changes and dissimilarities in LV systolic function, infarct size, cardiac remodeling, and wall motion abnormalities between the groups of mice eating the experimental diet (3.75 and 7.5 g/kg

OLT1177) and mice eating the standard diet. In addition to the 3-day echocardiography, TTE was also performed at 4-weeks and 10-weeks post-AMI. The echocardiography system that was used in this study was the Vevo770 High Resolution in vivo micro-imaging system (VisualSonics Inc, Toronto, Ontario) along with a transducer probe with a high transmit frequency of 30-MHz (Respress & Wehrens, 2010). Note: for comparison, the typical range of frequencies used in adult human echocardiography ranges from 2.0 to 5.0 MHz (Mitchell et al., 2019)

On days when transthoracic echocardiography was performed, each mouse was mildly anesthetized with pentobarbital (30-50 mg/kg) and shaved at the upper and lower chest area. Following this, the mouse was secured and placed in a supine position on a warmed VEVO770 platform. While in the supine position the investigator, that performed and read all echocardiograms, applied warmed ultrasound transmission gel on the animal's chest to enhance TTE image quality and next placed the transducer on the thoracic region to visualize the heart from the parasternal short-axis view (Note: this investigator was blinded to treatment allocation).

While echocardiography has three different imaging modes (B-mode, M-mode, and Doppler tissue imaging), for this study the animal's hearts were visualized using B-mode (2-D imaging). When the transducer was appropriately placed to see the parasternal short-axis (PSAX) view, B-mode reliably produced grayscale maps/images of the heart that allowed us to visualize ventricular wall motion abnormalities associated with infarcted myocardium (Lilly, 2013) and estimate the size of the left ventricle (Mitchell et al., 2019). Estimating the size of the LV is especially useful in assessing LV systolic function and cardiac enlargement (dilatation), thereby allowing researchers and clinicians a way to monitor pathophysiologies and responses to treatment in diseased hearts. From these images and M-mode tracing (Doppler data) the

parameters that were evaluated were the left ventricular end-diastolic diameter (LVEDD) and left ventricular end-systolic diameter (LVESD).

The manner in which infarct size and regional myocardial function were visually assessed was by evaluating the regional wall motion and left ventricular (LV) wall thickening through the usage of the 16-segment model of the left ventricle (LV) that allowed us to assess LV wall motion and wall thickening (Pellikka et al., 2020). While other segmentation models are used clinically, like the 17-segment and 18-segment models, we utilized the 16-segment model which was recommended for studies assessing wall motion and not segments located at the tip of the apex, whose wall would be imperceptible in our studies and thus irrelevant (R. Lang, L. Badano, V. Mor-Avi, J. Afilalo, A. Armstrong, 2015).

Through this 16-segment model, the investigator individually counted, analyzed, and graded the function of the 16-segments of the LV, giving a score of either 3 or 4 according to a 4-grade scoring system. This is especially useful when making visual assessments of LV myocardial regions that are supplied by occluded coronary arteries and identified by the reduction in motion (hypokinesis) or lack thereof (akinesis) in an ischemic, infarcted, or scarred myocardial wall region (R. Lang, L. Badano, V. Mor-Avi, J. Afilalo, A. Armstrong, 2015). The grades from this 16-segment model are described in Table 2. By averaging the scores of all segments visualized, a wall motion score index was produced and used to estimate the size of the infarct (Pellikka et al., 2020).

Score	Wall Motion	Endocardial Motion	Systolic Increase in Thickness
1	Normal	Normal	>50%
2	Hypokinetic	Reduced	<40%
3	Akinetic	Absent	<10%
4	Dyskinetic	Outward/Paradoxical	Thinning

Table 2: The 4-grade scoring system utilized alongside the 16-segment model. (Pellikka et al., 2020).

During these LV wall thickening readings, an investigator also utilized a cursor on the echo system screen to mark the location of the endocardial border during diastole and assess the change that occurs to LV wall thickening during systole, which helped in estimating the thickness of the LV wall. (Pellikka et al., 2020). From these images and M-mode tracing (Doppler data), the parameters that were evaluated included anterior wall diastolic thickness (AWDT), posterior wall diastolic thickness (PWDT), anterior wall systolic thickness (AWST), and posterior wall systolic thickness (PWST).

The left ventricular structural parameters that were visually assessed with the use of TTE were also utilized to calculate left ventricular fractional shortening (FS), ejection fraction (EF), and LV mass.

LV fractional shortening is a calculated parameter that measures the functional capacity that the heart is able to squeeze/contract. It was calculated utilizing the following formula:

$$LVFS = (LVEDD-LVESD) / LVEDD \times 100$$

LV Ejection fraction is a measure of contractile function and it was calculated with the Teichholz formula. To measure the left ventricular ejection fraction, the measured LV end-diastolic and end-systolic areas were measured with B-mode TTE and converted to volumes LVESV and LVEDV. With these values the following formula is capable of calculating LVEF:

$$LVEF = (EDV - ESV) / EDV \times 100$$

However, when it comes to changes in shape from a physiologically ellipsoid to an adverse dilated shape, the LVEF was derived utilizing the Teicholz formula, a formula dependent on estimating LV end-systolic and end-diastolic volumes to the third power of the diameter multiplied by a factor of 1.047 according to the ellipsoid shape in which the length is twice the diameter: (Toldo et al., 2019).

$$LVEF = [LVEDD^3 - LVESD^3] / LVEDD^3$$

LV mass is a strong predictor of cardiovascular events that is also calculated utilizing M-mode echocardiography parameters. Although there are several methods that can calculate the LV mass, the method that was utilized in this study was the Linear Method. Through the Linear Method, LV mass was calculated utilizing the Cube Formula, a geometric formula that incorporates the 2D echocardiography linear measurements of LV diastolic diameter and wall thickness to first calculate the volume of the LV myocardium. Then it converts the volume to mass by multiplying the volume of LV myocardium by the myocardial density (approx.1.05 g/mL in humans)(R. Lang, L. Badano, V. Mor-Avi, J. Afilalo, A. Armstrong, 2015)

$$LV\ mass = 0.8 \cdot 1.04 \cdot [(IVS + LVID + PWT)^3 - LVID^3] + 0.6g$$

Note: IVS, interventricular septum; LVID, left ventricle internal diameter; PWT, inferolateral wall thickness.

2.4 Isoproterenol Challenge

Immediately following the 4-week and 10-week echocardiogram, isoproterenol (20 ng/mouse) was injected intraperitoneally to each anesthetized mouse while in the supine position on the VEVO770 platform for the purpose of assessing myocardial contractile reserve.

Furthermore, at this point in the 10-week study all mice that underwent a permanent ligated nonreperfused AMI would have also experienced adverse cardiac remodeling leading to heart failure. As mentioned previously, cardiac remodeling is regulated by neurohormonal, RAAS, and inflammatory signaling pathways, that are initially beneficial, but as time passes becomes maladaptive leading to adverse ventricular remodeling and heart failure. Additionally, as cardiac efficiency diminishes significant desensitization and downregulation of ß-adrenergic receptors occurs leading to reduced responsiveness of the ß-adrenergic receptor system and loss of contractility (Lohse et al., 2003).

Isoproterenol is a potent, synthetic β-adrenergic receptor agonist that has positive chronotropic (increased HR) and inotropic (increased contractility) properties. As a result, we utilized isoproterenol to characterize OLT1177's effect on preserving systolic function, contractile reserve, and ß-adrenergic sympathetic responses in OLT-treated mice. Through the use of TTE, measurements were taken to calculate the percent increase in EF (contractile reserve) and LVFS within 5 minutes after isoproterenol injection.

2.5 LV Catheterization Procedure

Eight days after the 10-week TTE, all surviving mice underwent LV catheterization, a terminal procedure that was utilized to evaluate LV function in vivo.

In preparation for this procedure, all mice were anesthetized with pentobarbital (50-70 mg/kg) and shaved at the anterior neck region. After the preparation of the mice and surgical environment, incisions were made in the neck area of each mouse. These incisions exposed the vasculature of the neck area particularly the carotid arteries. Next, a pressure probe catheter (Millar Inc., Houston, TX), also known as a Millar® Mikro-Tip® Pressure Transducer Catheter,

was inserted into the right carotid artery and was further driven to the left ventricle of the heart to measure intracardiac pressure-volume tracings. Additionally, when a catheter is inserted into a blood vessel leading to the heart, each cardiac chamber produces a characteristic pressure-volume loop that is important in both locating the position of the probe catheter, as well as deriving important in vivo physiologic information. Although the probe catheter is small, it was extremely intricate and helpful in allowing us to measure and record the Peak systolic pressures (PSP), LV end-diastolic pressures (LVEDP), and velocity of contraction and relaxation ($+dP/dt$ and $-dP/dt$). Furthermore, the values from this probe catheter were recorded (in real-time) and measured using Labchart Pro 5 (Millar Inc., Houston, TX).

2.6 Timeline of the Study Protocol
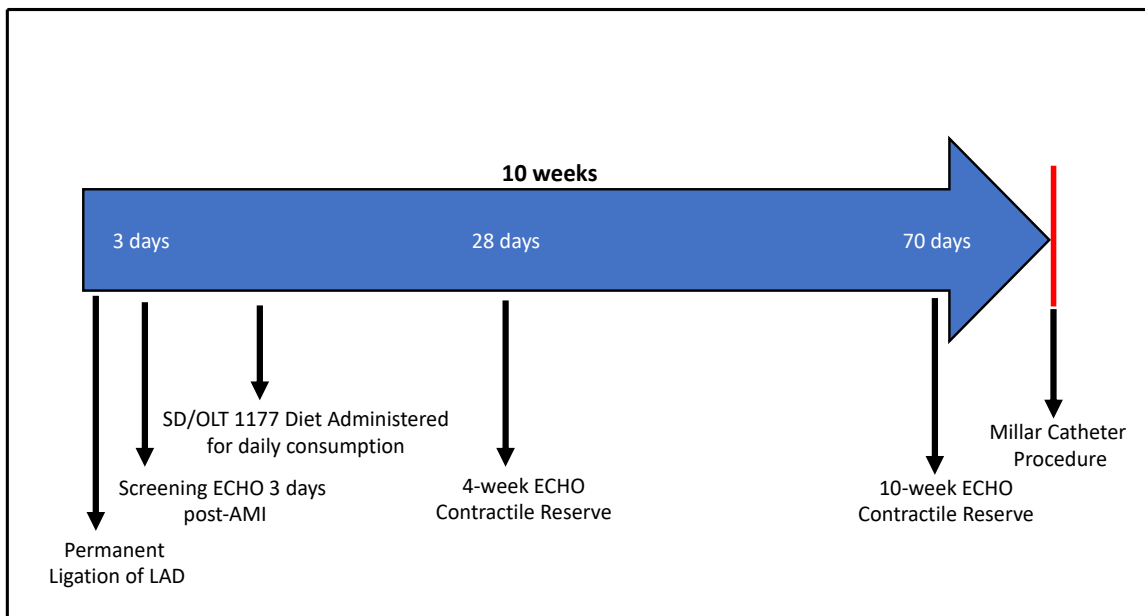
Figure 8: Timeline of the study protocol. LAD, Left anterior descending artery; SD, standard diet; ECHO, echocardiography; contractile reserve, isoproterenol challenge.

2.7 Statistical Analysis

All data presented in the following chapter utilized values derived from the procedures and techniques explained in this chapter. Additionally, the values from these procedures and techniques are presented as the mean and standard error of the mean. The differences between mouse treatment groups were compared by utilizing two-tailed Student's T-test. One-way analysis of variance (ANOVA) was used for the comparison of two different doses and the control condition with post-hoc Bonferroni's test for multiple comparisons. Unadjusted p-values are reported throughout, with statistical significance set at the 2-tailed 0.05 level (≤ 0.05).

CHAPTER 3: Results

3.1 The Effects of OLT1177 on Systolic Function

The left ventricular ejection fraction (LVEF) of all surviving mice were measured 3 days, 4-weeks, and 10-weeks post-AMI through the use of transthoracic echocardiography (TTE). From these TTE measurements measuring LVEF at 3-days post-AMI (Figure 9), we see a marked decrease in systolic function, as evidenced by the low mean LVEF ($27.6 \pm 0.9\%$) and LVFS ($12.9 \pm 0.4\%$) of all mice groups that underwent permanent ligation of the left anterior descending coronary artery (Table 3, 4, and 5). Whereas the mice group that underwent the sham operation maintained normal ejection fractions ($64.3 \pm 2.1\%$) and LV fractional shortening ($34.8 \pm 1.6\%$). After the assessment of the initial 3-day ECHO values, these mice were assigned to four different groups.

Based on TTE measurement comparisons at 3-days and at 10-weeks post-AMI (Figure 9) no significant differences in LVEF were noted between the OLT-treated mice groups and the control diet mice group. Additionally, both low- and high-dose OLT-treated experimental groups showed similar ejection fractions and downward trends in LVEF when compared to the control group ($22.6 \pm 1.8\%$ in OLT 3.75gr/kg or $24.7 \pm 3.1\%$ in OLT 7.50gr/kg vs $21.9 \pm 1.9\%$ in control group, $P = 0.77$, $P = 0.44$) (Figure 10). Therefore, these data indicate that OLT1177 had no significant effect on the LVEF of OLT-treated mice.
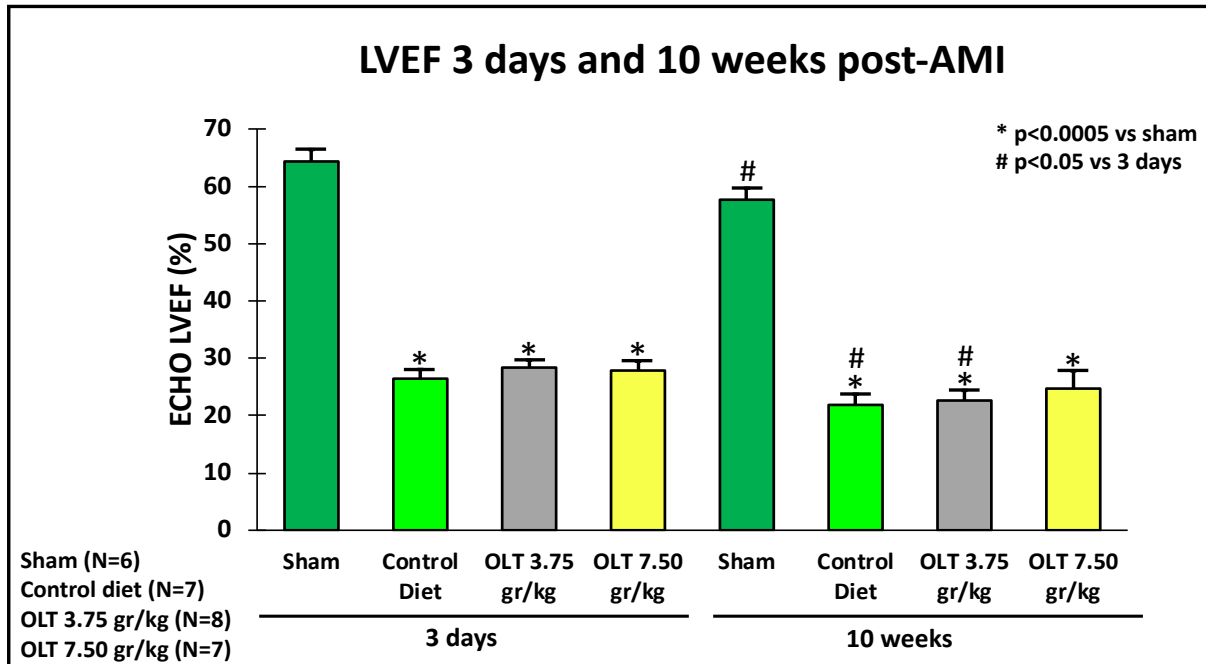
Figure 9: LVEF, Left ventricular ejection fraction at 3-days and 10-weeks after permanent ligation of the LAD coronary artery.
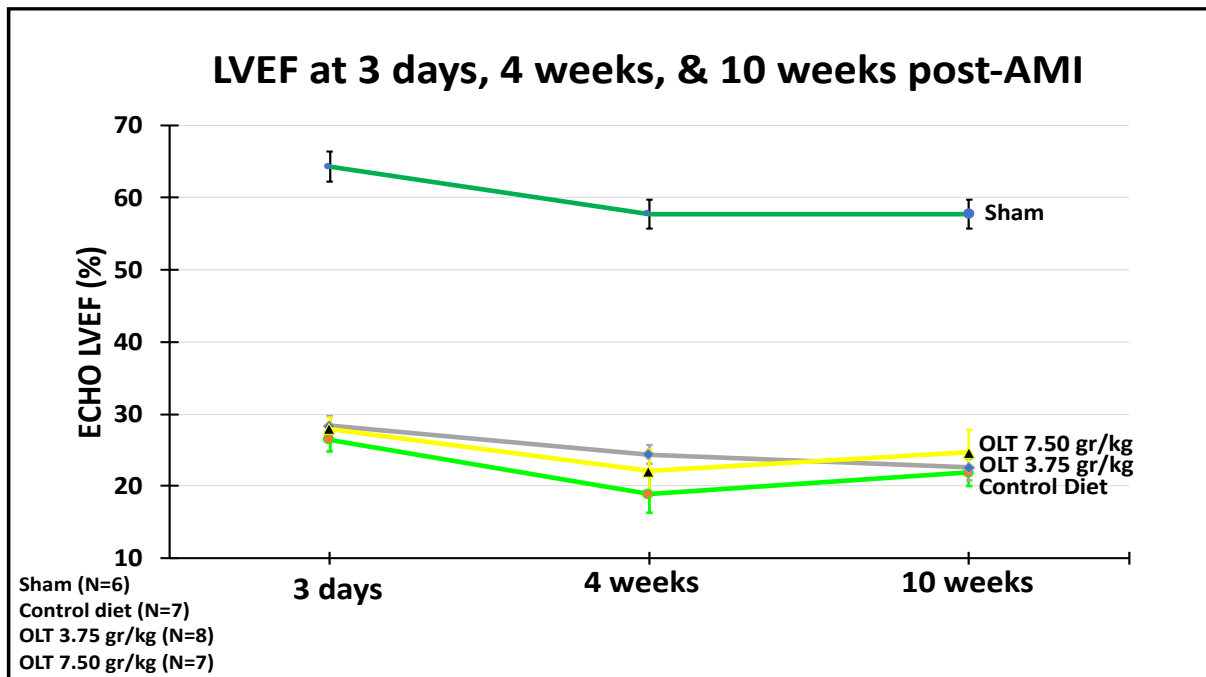
Figure 10: LVEF, Left ventricular ejection fraction at 3-days, 4-weeks, and 10-weeks post-AMI scatter plot

3.2 The Effects of OLT1177 on Cardiac Remodeling

As expected, TTE measurements acquired at 3-days post-AMI show pronounced cardiac remodeling in the form of LV dilatation and eccentric LV hypertrophy, as evidenced by the significant increase in LVEDD, LVESD, and LV mass in all mice that underwent permanent ligation of the left anterior descending coronary artery (Figure 11, 13, 15). Whereas sham-operated mice, when compared to treatment and control groups displayed a significantly preserved LVEDD, LVESD, and LV mass, thus no cardiac remodeling.

LVEDD:

TTE parameters measured throughout the 10-week study show that both OLT-treated mice groups and control group mice, when compared to the sham group, had significant increases in LVEDD after 10 weeks: control group mice (6.38 ± 0.26mm vs 4.07 ± 0.10mm, $P < 0.0005$), low dose OLT group mice (5.71 ± 0.16 vs 4.07 ± 0.10mm, $P < 0.0005$), and high dose OLT group mice (6.13 ± 0.22 vs 4.07 ± 0.10mm, $P < 0.0005$) as seen in Figure 11.
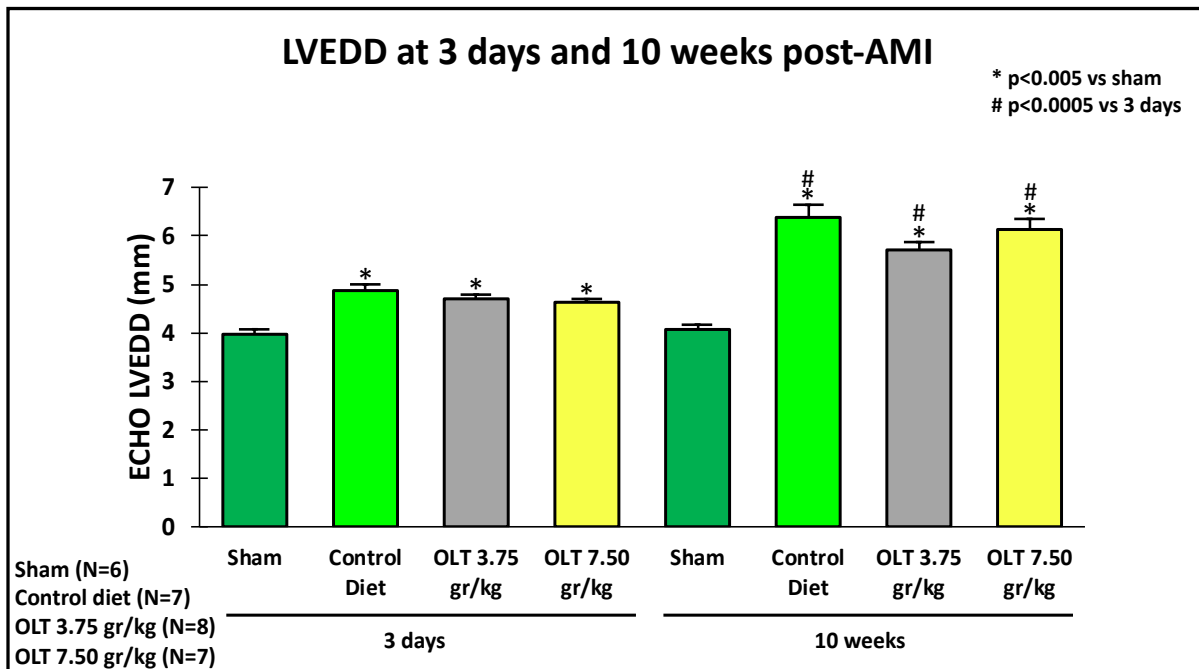
Figure 11: LVEDD, Left ventricular end diastolic diameter at 3-days and 10-weeks after permanent ligation of the left anterior descending coronary artery.

Additionally, both low- and high-dose OLT-treated experimental groups displayed a similar upward trend in LVEDD when compared to the control group (Figure 12). LVEDD TTE measurements after 10 weeks suggests that both OLT-treated mice groups, when compared to the control group, did not significantly attenuate ventricular enlargement.
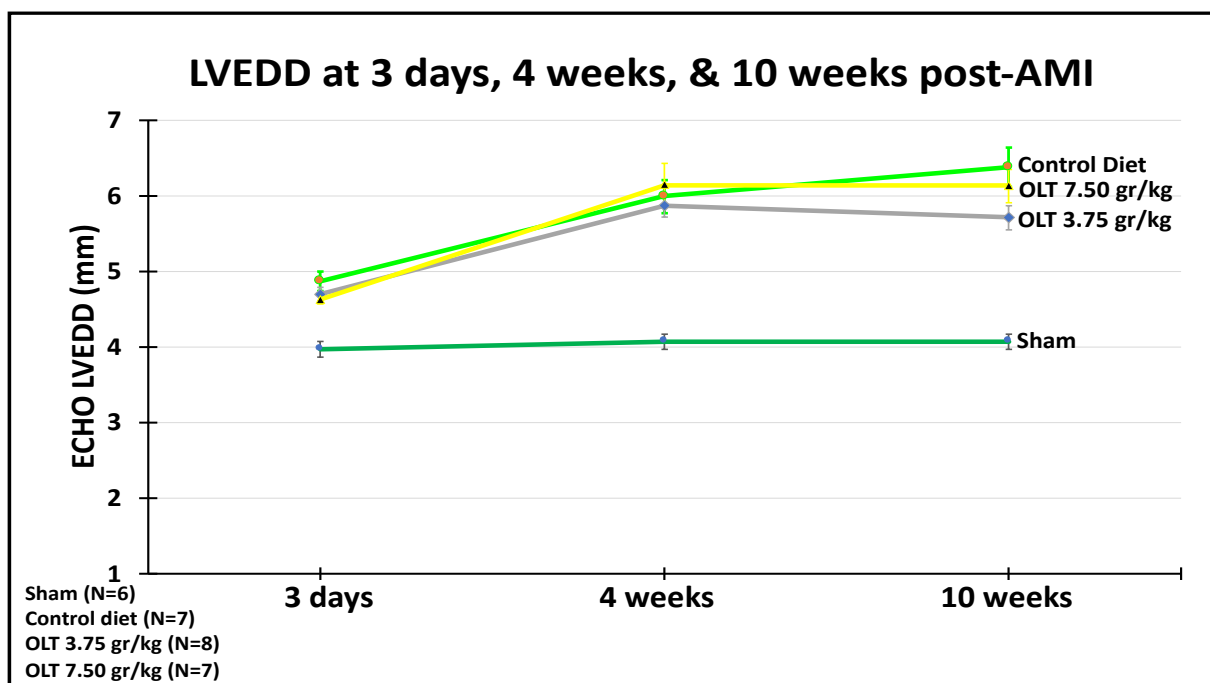
Figure 12: LVEDD, Left ventricular end diastolic diameter at 3-days, 4-weeks and 10-weeks after AMI surgery.

LVESD:

TTE parameters measured at 3 days and 10 weeks after permanent ligation surgery show that both OLT-treated mice groups and control diet group mice had similar and significant percent increases in LVESD: control group mice (+33%, $P < 0.0005$), low dose OLT group mice (+30%, $P < 0.0005$), and high dose OLT group mice (+35%, $P < 0.0005$) as seen in Figure 13.
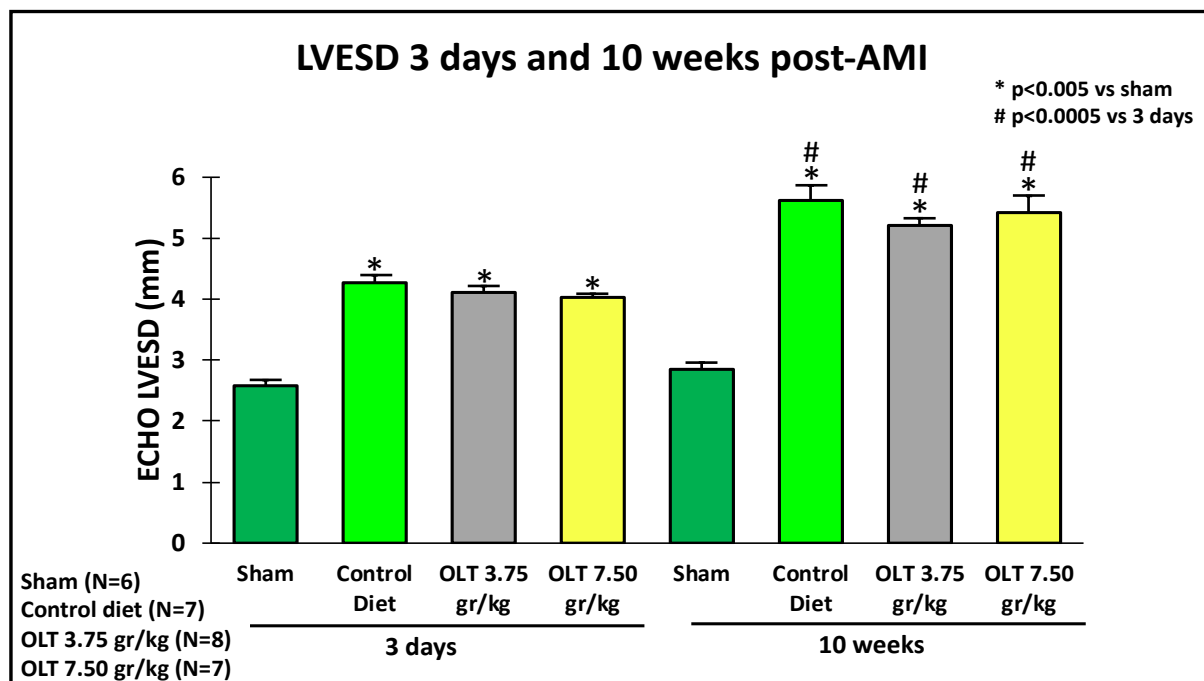
Figure 13: LVESD, Left ventricular end systolic diameter at 3-days and 10-weeks after permanent ligation of the left anterior descending coronary artery
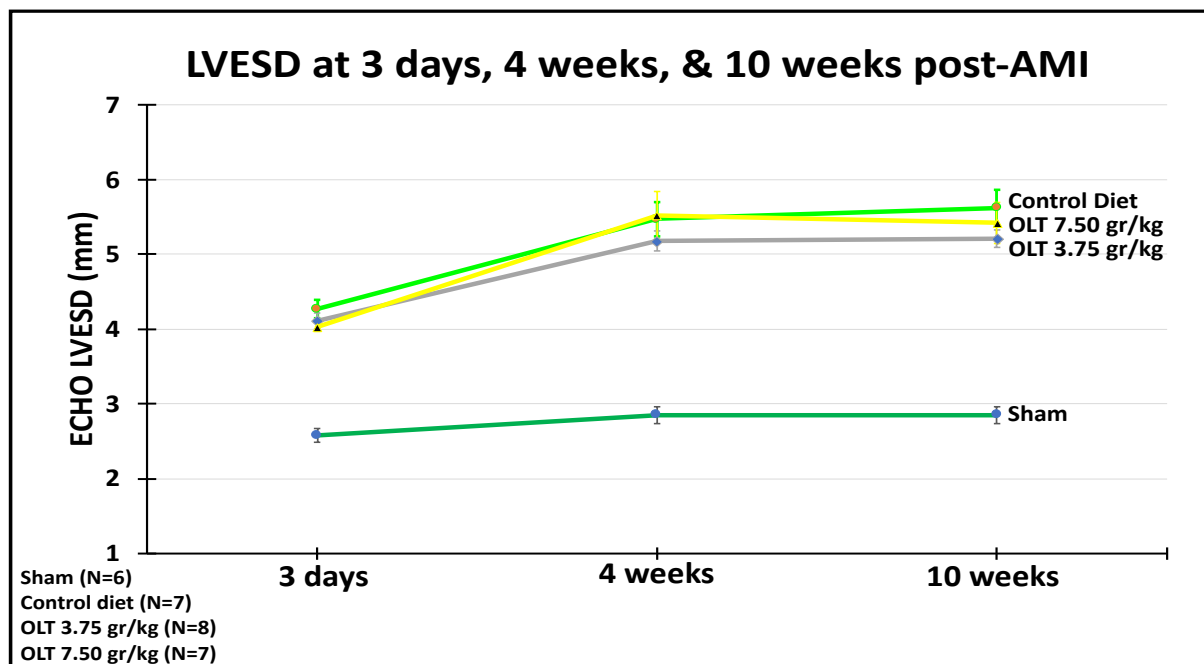
Figure 14: LVESD, Left ventricular end systolic diameter at 3-days, 4-weeks, and 10-weeks after nonreperfused AMI surgery.

LVESD TTE measurement after 10 weeks also demonstrated that neither low dose OLT-treated mice (3.75gr/kg OLT), nor high dose OLT-treated mice (7.50gr/kg) had a significant effect on attenuating ventricular enlargement in relation to LVESD when compared to the control group (5.21 $\pm$ 0.12mm in OLT 3.75gr/kg or 5.42 $\pm$ 0.28mm in OLT 7.5 gr/kg vs 5.62 $\pm$ 0.24mm control group, P = 0.13 and P = 0.58 respectively) (Figure 13, 14).

Calculated LV Mass:

TTE measurements also allowed us to utilize ECHO values to calculate left ventricular mass. TTE parameters measured at 3 days post-AMI (Figure 15) show that both OLT-treated mice groups and control diet group mice, when compared to ECHO values measured at 10 weeks post-AMI, had significant increase in LV mass: control group mice (110.5 $\pm$ 6.0mg vs 187.1 $\pm$ 13.5mg, P < 0.05), low dose OLT group mice (104.4 $\pm$ 3.4mg vs 157.5 $\pm$ 12.1mg , P < 0.05), and high dose OLT group mice (96.5 $\pm$ 6.3 vs 180.4 $\pm$ 17.5mg, P < 0.05). Similarly, from Figure 16, we see that the high-dose OLT-treated mice group and the control diet group show a similar upward trend in LV mass throughout the 10-week study. Figure 16 also appears to show a somewhat attenuated LV mass in low-dose OLT-treated mice, however this finding was not significant when compared to the control group.

All things considered, Figure 15 shows that when comparing both OLT-treated mice groups to the control group, OLT1177 had no significant effect on attenuating the gradual increase in LV mass that occurs throughout the 10-week study.
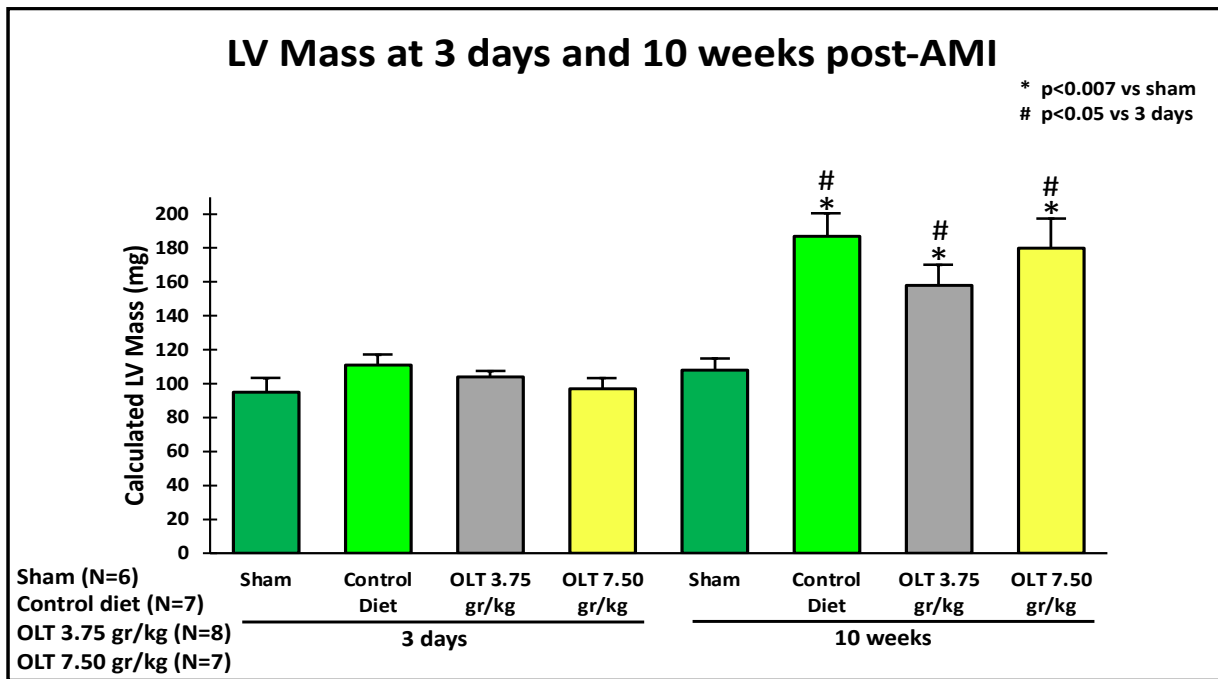
Figure 15: Calculated LV Mass at 3-days and 10-weeks after permanent ligation of the left anterior descending coronary artery.
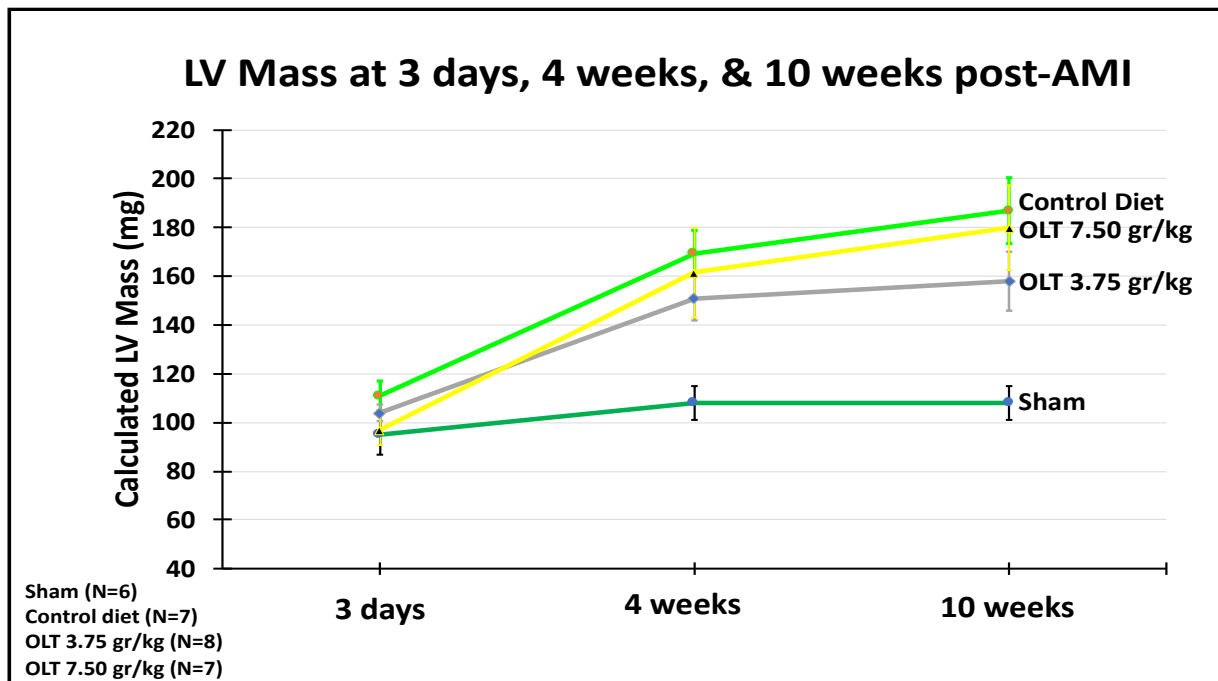
Figure 16: Calculated LV Mass at 3-days, 4-weeks and 10-weeks after permanent ligation surgery

The significant increase in LV mass of all mice groups that underwent nonreperfused AMI surgery, indicates that cardiac remodeling in the form of LV hypertrophy has occurred (Figure 15 and 16). To determine whether concentric or eccentric LV hypertrophy occurred, TTE measurements of LV mass along with LV diameters (LVEDD and LVESD) were evaluated.

Based on these ECHO values, we determined that both OLT-treated mice groups and the control diet group underwent eccentric LV hypertrophy, as evidenced by the increase in LV mass along with an increase in diameters (LVEDD, LVESD) seen in Tables 3, 4, and 5. The increase in the diameter or cavity of the left ventricle, as previously discussed, initially allows the heart to accommodate more blood volume in order to maintain stroke volume and cardiac output. However, as time passes, the continual increase in blood volume can lead to eccentric hypertrophy and volume overload associated with systolic heart failure. On the other hand, had TTE measurements shown that LV mass increased while the diameter (LVEDD) had not, it would have been indicative of concentric LV hypertrophy resulting from significant thickening of the heart muscle in the left ventricle.

Further evidence of Eccentric remodeling was paralleled by calculating the index of Eccentric Remodeling:

Index of Eccentric Remodeling = (AWDT + PWDT) / LVEDD

Sham operated mice: $(0.86 + 0.88) / 4.07 = 0.427$

Control group mice: $(0.47 + 0.99) / 6.38 = 0.229$

Low dose OLT-treated mice: $(0.47 + 1.01) / 5.71 = 0.259$

High dose OLT-treated mice: $(0.51 + 0.98) / 6.13 = 0.229$

By inputting the corresponding TTE values seen in Tables 3, 4, 5, and 6 into the formula we see that all mice groups that underwent nonreperfused AMI surgery display a lower index of eccentric remodeling (when compared to sham operated mice) demonstrating an increase in LV diameter along with a thinner LV wall. Thus, further indicating that eccentric LV hypertrophy had occurred.

Table 3: Left Ventricular Structural Parameters of Group 1 Mice (MI + 3.75g/kg OLT Diet)

	3 days post-AMI	4 wks post-AMI	10 wks post-AMI	% Change (3d to 10wks)
N=	8	8	8	8
EDD (mm)	4.63 ± 0.16	5.87 ± 0.42	5.71 ± 0.46	23.3% ↑
ESD (mm)	4.02 ± 0.20	5.18 ± 0.38	5.21 ± 0.33	29.6% ↑
AWDT (mm)	0.55 ± 0.06	0.42 ± 0.04	0.47 ± 0.08	-14.5% ↓
PWDT (mm)	0.89 ± 0.08	0.97 ± 0.20	1.01 ± 0.08	13.5% ↑
AWST (mm)	0.57 ± 0.06	0.42 ± 0.04	0.48 ± 0.10	-15.8% ↓
PWST (mm)	1.30 ± 0.15	1.40 ± 0.24	1.40 ± 0.12	7.70% ↑
FS (%)	13.5 ± 1.77	11.6 ± 1.92	10.5 ± 2.45	-22.2% ↓
EF (%)	28.4 ± 3.66	24.4 ± 3.74	22.6 ± 4.96	-20.4% ↓
HR (bpm)	379.9 ± 50.4	316.3 ± 77.1	311.5 ± 51.2	-18.0% ↓
Calc. LV Mass (mg)	104.4 ± 9.54	151.0 ± 25.7	157.5 ± 34.3	50.0% ↑

Note: Values are Mean ± SD; EDD, End diastolic diameter; ESD, End systolic diameter; AWDT, anterior wall diastolic thickness; PWDT, posterior wall diastolic thickness; AWST, anterior wall systolic thickness; PWST, posterior wall systolic thickness; FS, fractional shortening; EF, ejection fraction; HR, heart rate.

Table 4: Left Ventricular Structural Parameters of Group 2 Mice (MI + 7.50g/kg OLT Diet)

	3 days post-AMI	4 wks post-AMI	10 wks post-AMI	% Change (3d to 10wks)
N=	7	7	7	7
EDD (mm)	4.61 ± 0.17	6.14 ± 0.77	6.13 ± 0.58	33.0% ↑
ESD (mm)	4.01 ± 0.17	5.52 ± 0.85	5.42 ± 0.73	35.2% ↑
AWDT (mm)	0.55 ± 0.07	0.46 ± 0.07	0.51 ± 0.06	-7.27% ↓
PWDT (mm)	0.81 ± 0.16	0.89 ± 0.19	0.98 ± 0.16	21.0% ↑
AWST (mm)	0.58 ± 0.08	0.47 ± 0.08	0.51 ± 0.07	-12.1% ↓
PWST (mm)	1.17 ± 0.23	1.17 ± 0.25	1.39 ± 0.23	18.8% ↑
FS (%)	13.0 ± 2.00	10.1 ± 3.85	11.9 ± 4.10	-8.46% ↓
EF (%)	27.9 ± 4.34	22.1 ± 7.88	24.7 ± 8.20	-11.5% ↓
HR (bpm)	439.4 ± 61.3	305.7 ± 60.7	334.0 ± 45.9	-24.0% ↓
Calc. LV Mass (mg)	96.5 ± 16.7	161.6 ± 49.0	180.4 ± 46.2	86.9% ↑

Note: Values are Mean ± SD; EDD, End diastolic diameter; ESD, End systolic diameter; AWDT, anterior wall diastolic thickness; PWDT, posterior wall diastolic thickness; AWST, anterior wall systolic thickness; PWST, posterior wall systolic thickness; FS, fractional shortening; EF, ejection fraction; HR, heart rate.

Table 5: Left Ventricular Structural Parameters of Group 3 Mice (MI + SD Diet) i.e. Control

	3 days post-AMI	4 wks post-AMI	10 wks post-AMI	% Change (3d to 10wks)
N=	7	7	7	7
EDD (mm)	4.83 ± 0.41	5.99 ± 0.58	6.38 ± 0.69	32.1% ↑
ESD (mm)	4.24 ± 0.37	5.47 ± 0.61	5.62 ± 0.64	32.5% ↑
AWDT (mm)	0.53 ± 0.07	0.49 ± 0.11	0.47 ± 0.08	-11.3% ↓
PWDT (mm)	0.89 ± 0.11	1.00 ± 0.20	0.99 ± 0.14	11.2% ↑
AWST (mm)	0.55 ± 0.06	0.53 ± 0.24	0.45 ± 0.08	-18.2% ↓
PWST (mm)	1.29 ± 0.19	1.37 ± 0.17	1.39 ± 0.21	7.75% ↑
FS (%)	12.1 ± 2.19	8.43 ± 3.20	10.4 ± 2.30	-14.1% ↓
EF (%)	26.4 ± 4.28	18.9 ± 6.84	21.9 ± 4.95	-17.1% ↓
HR (bpm)	400.0 ± 55.6	351.7 ± 62.8	312.1 ± 56.2	-22.0% ↓
Calc. LV Mass (mg)	110.5 ± 16.0	169.5 ± 25.0	187.2 ± 35.7	69.4% ↑

Note: Values are Mean ± SD; EDD, End diastolic diameter; ESD, End systolic diameter; AWDT, anterior wall diastolic thickness; PWDT, posterior wall diastolic thickness; AWST, anterior wall systolic thickness; PWST, posterior wall systolic thickness; FS, fractional shortening; EF, ejection fraction; HR, heart rate.

Table 6: Left Ventricular Structural Parameters of Group 4 Mice (Sham + SD Diet)

	3 days post-AMI	4 wks post-AMI	10 wks post-AMI	% Change (3d to 10wks)
N=	6	6	6	6
EDD (mm)	3.97 ± 0.26		4.07 ± 0.25	2.52% ↑
ESD (mm)	2.58 ± 0.22		2.85 ± 0.28	10.5% ↑
AWDT (mm)	0.80 ± 0.09		0.86 ± 0.09	7.50% ↑
PWDT (mm)	0.83 ± 0.09		0.88 ± 0.08	6.02% ↑
AWST (mm)	1.28 ± 0.10		1.27 ± 0.10	-0.78% ↓
PWST (mm)	1.20 ± 0.12		1.29 ± 0.15	7.50% ↑
FS (%)	34.8 ± 3.97		30.2 ± 3.49	-13.2% ↓
EF (%)	64.3 ± 5.13		57.7 ± 4.93	-10.3% ↓
HR (bpm)	407.8 ± 78.7		413.0 ± 87.3	1.28% ↑
Calc. LV Mass (mg)	95.3 ± 20.1		107.6 ± 17.0	12.9% ↑

Note: Values are Mean ± SD; EDD, End diastolic diameter; ESD, End systolic diameter; AWDT, anterior wall diastolic thickness; PWDT, posterior wall diastolic thickness; AWST, anterior wall systolic thickness; PWST, posterior wall systolic thickness; FS, fractional shortening; EF, ejection fraction; HR, heart rate.

3.3 The Effects of OLT1177 on Contractile Reserve

Throughout this 10-week study, LV contractile reserve / ß-adrenergic response was measured twice as a percent change at 4-weeks and 10-weeks post-AMI. At 4-weeks post-AMI, both experimental OLT-treated mice groups and the control diet group were administered isoproterenol (i.p.) immediately following TTE assessment. From Figure 17 we see that both OLT-treated mice groups 3.75 gr/kg OLT and 7.50gr/kg OLT (when compared to the control group) had noticeably greater contractile reserve and thus greater ß-adrenergic responses to isoproterenol (+26 ± 11% vs +14 ± 10%, P<0.46) and (+31 ± 10% vs +14 ± 10%, P < 0.27) respectively. Whereas control diet mice exhibited a blunted ß-adrenergic response to isoproterenol (+14 ± 10%).
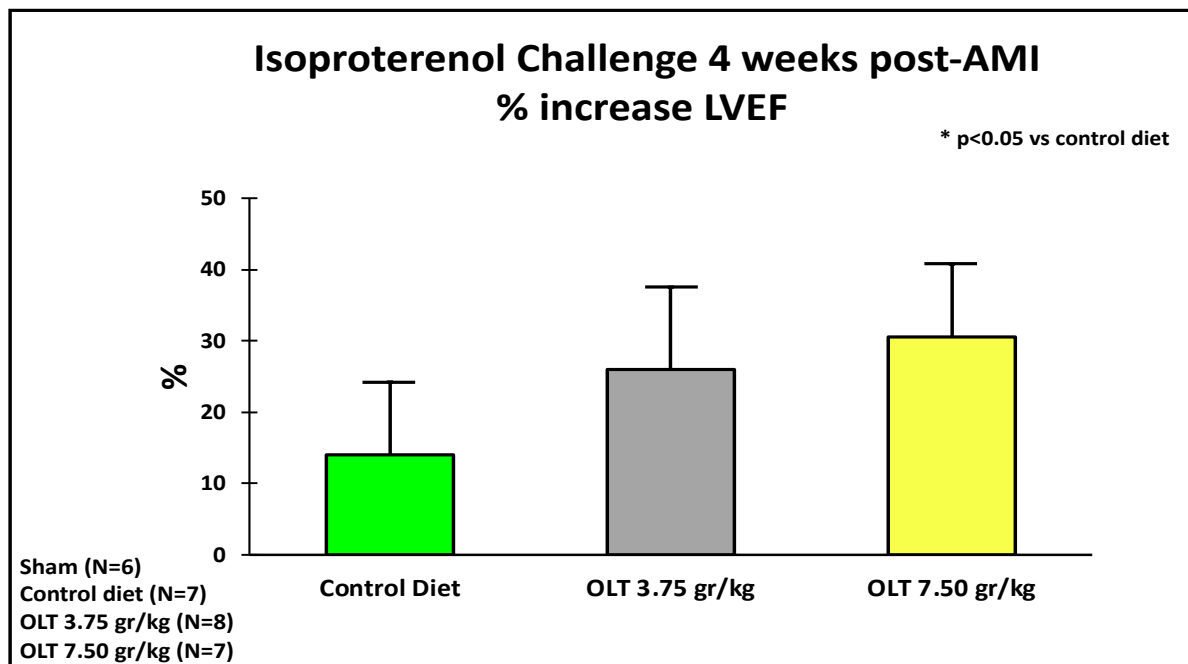
Figure 17: Contractile reserve assessment at 4 weeks after nonreperfused AMI surgery.

At 10-weeks post-AMI, both OLT-treated mice groups, the control group, and sham-operated mice were administered isoproterenol i.p. immediately following TTE assessment. From Figure 18 and 19 we see that low dose OLT-treated mice (3.75 gr/kg OLT) when compared to the control group mice displayed a significantly greater ß-adrenergic response and LVEF percent increase ($33 \pm 11\%$ vs $9 \pm 7\%$ P < 0.05) and LVFS percent increase ($34 \pm 10\%$ vs $4 \pm 6\%$, P < 0.05). Figure 18 also shows that high dose OLT-treated mice (7.50 gr/kg OLT) when compared to control diet group mice displayed a significantly greater ß-adrenergic response and LVEF percent increase ($40 \pm 6\%$ vs $9 \pm 7\%$, P < 0.005) and LVFS percent increase ($41 \pm 7\%$ vs $4 \pm 6\%$, P < 0.005) (Figure 19). Whereas the control diet mice, when compared to sham-operated mice, exhibited a significantly blunted ß-adrenergic response to isoproterenol ($9 \pm 7\%$ vs $28 \pm 4\%$ LVEF, P<0.05). The significant percent increases of LVEF and LVFS, which were seen in both OLT-treated mice groups when compared to the control group, suggests that OLT1177 had a significant effect on restoring the contractile reserve and ß-adrenergic response after AMI surgery.
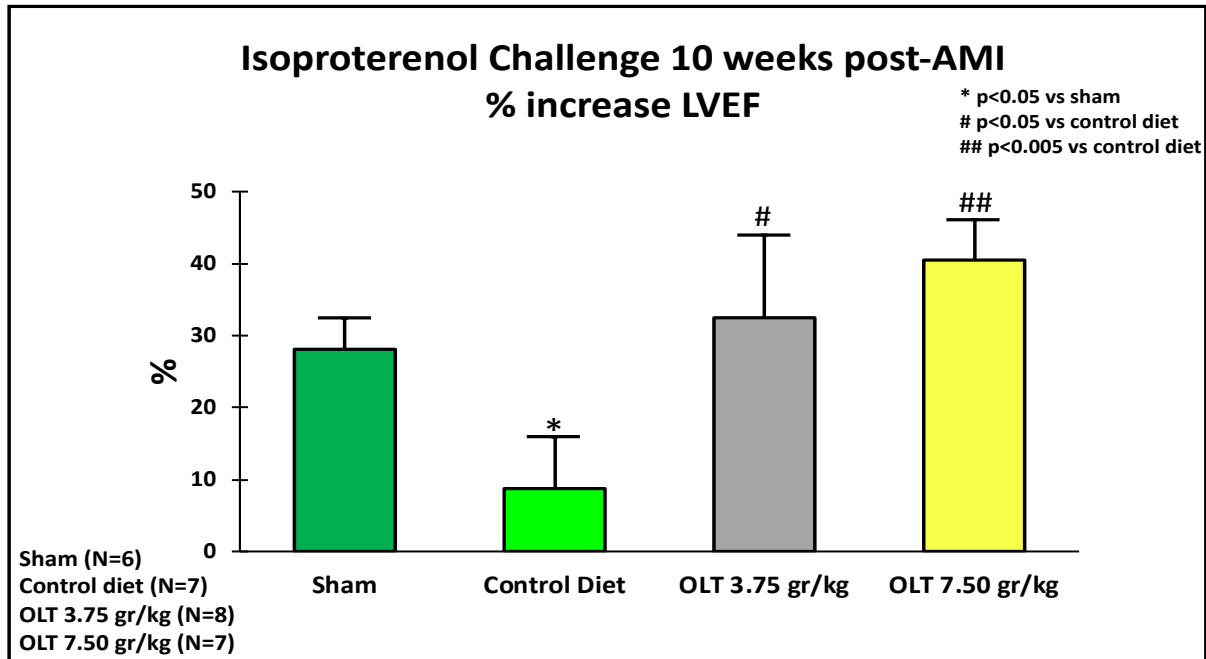
Figure 18: LVEF Contractile reserve assessment at 10 weeks after nonreperfused AMI surgery.
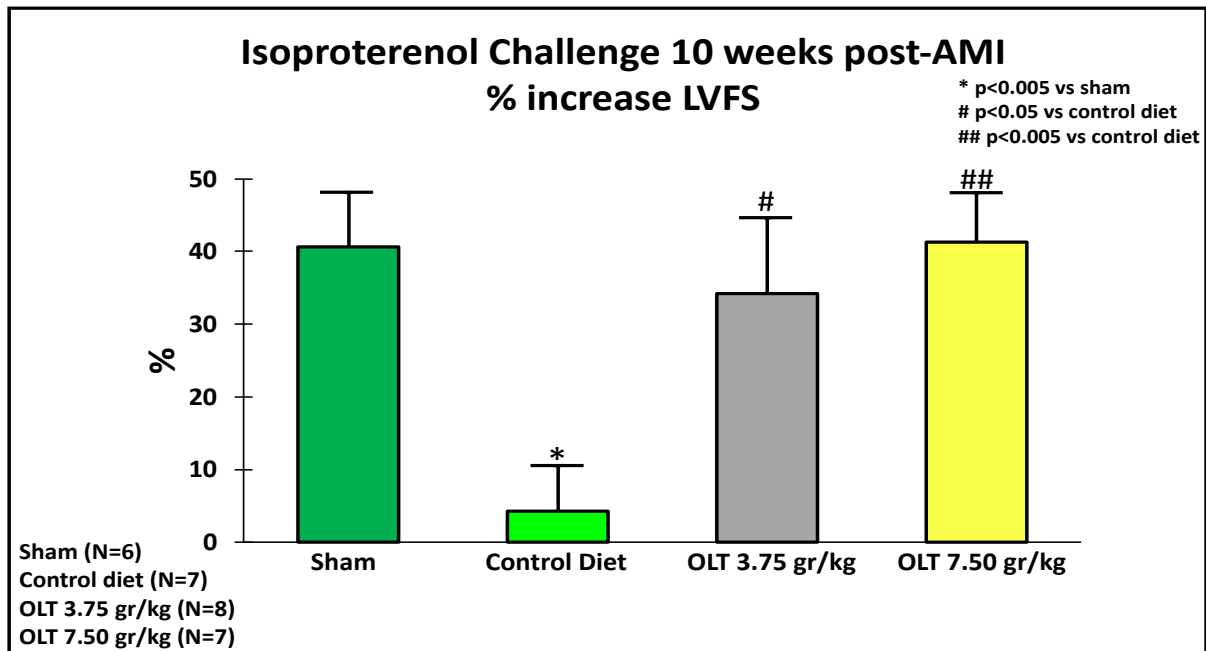
Figure 19: LVFS Contractile reserve assessment at 10 weeks after nonreperfused AMI surgery.

3.4 The Effects of OLT1177 on Diastolic Function

Eight days after the 10-week TTE assessment, the cardiac function of all surviving mice

was assessed with the use of LV catheterization (Note: some mice [n=5] did not survive long

enough to record LV catheterization values during this procedure). The principle parameter that

was measured was LV end diastolic pressure (LVEDP).

From these LV catheterization measurements (Figure 20), we see a greater degree of

diastolic dysfunction in control group mice, as evidenced by the significantly higher LVEDP

(10mmHg) displayed in comparison to all other mice groups.
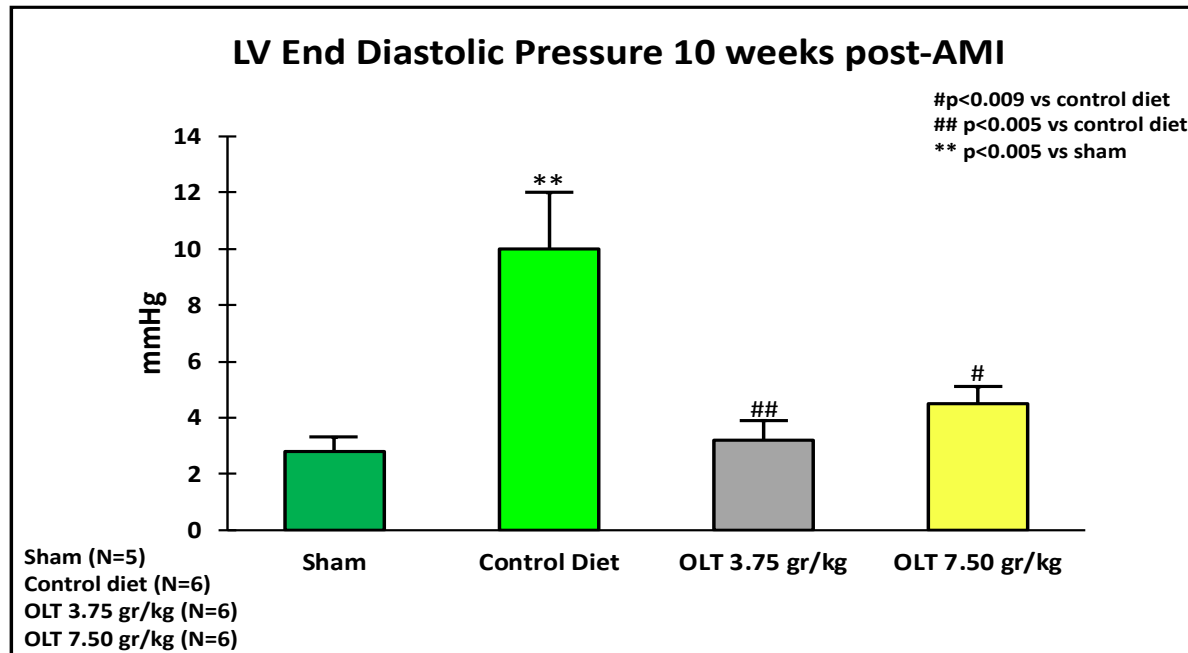
Figure 20: LV catheterization assessment of LVEDP, LV end diastolic pressure at ∼11 weeks after nonreperfused AMI surgery.

Figure 20 also demonstrates that both OLT-treated mice groups (3.75 gr/kg OLT and 7.50gr/kg

OLT) and sham-operated mice displayed similar LV end-diastolic pressures. Thus, indicating

that treatment with OLT1177 3.75 gr/kg or 7.50 gr/kg led to the preservation of diastolic

function with a significantly lower LVEDP when compared to the control group (3.2 ± 0.5

mmHg, or 4.5 ± 0.5 mmHg vs 10.0 ± 1.6 mmHg in standard diet; $P < 0.005$ and $P < 0.009$).

All things considered, the elevated filling pressures (LVEDP) in control group mice, can

be an indicator of heart failure. Whereas, a lower or normal LVEDP seen in the OLT-treated

mice groups seem to suggest that OLT1177 treatment is effective at preventing the increase in filling pressure due to diastolic dysfunction.

3.5 Chapter Summary

The general aim of our study was to assess the effects of OLT1177 on improving cardiac function, cardiac remodeling, and contractile reserve. For this purpose, our experimental groups were fed an OLT1177-enriched diet (3.75g or 7.50g of OLT1177 per kg of food) starting 1 week after nonreperfused AMI surgery until the end of the 10-week experiment.

At the end of 10 weeks 2 of 10 mice (20%) mice had died in the OLT 3.75 gr/kg group, as compared with 2 of 9 mice (22%) in the OLT 7.5 gr/kg group, 3 of 10 mice (30%) in standard diet, and 0 of 6 (0%) in sham-operated mice. Our results from this study, taken from transthoracic echocardiography, isoproterenol challenge, and LV catheterization, show that control group mice (when compared to sham operated mice) displayed a significant increase in cardiac remodeling in the form of LV dilatation ([LVEDD] 6.4±0.3mm vs 4.07±0.1mm, P <0.0005) and eccentric LV hypertrophy ([LV mass] 187.1±13.5mg vs 107.6±6.9, P<0.0005), a significant decrease in systolic function as evidenced by a significantly reduced LVEF (21.9±1.9% vs 57.7±2.0%, P<0.0005), a significant loss in contractile reserve/ß-adrenergic response([%change in LVEF] 8.7±7.2% vs 28.1±4.3%, P<0.05), and a significant decrease in diastolic function in the form of increasing filling pressures ([LVEDP] 10.0±1.6mmHg vs 2.8±0.5mmHg, P<0.005)

Whereas data from our experimental mice groups treated with a 3.75 gr/kg or 7.50 gr/kg OLT1177 diet (when compared to the control group) suggests that OLT1177 treatment led to

restoration of contractile reserve (percent increase in LVEF after isoproterenol challenge ($33 \pm$ 11% or $40 \pm 6\%$ vs $+9 \pm 7$ % in standard diet; $P<0.05$ and $P<0.005$ respectively). Treatment with OLT 3.75 gr/kg or 7.5 gr/kg also led to preservation of diastolic function (left ventricular end-diastolic pressure 3.2 ± 0.5 mmHg, or 4.5 ± 0.5 mmHg vs 10.0 ± 1.6 mmHg in standard diet; $P<0.005$ and $P<0.009$). The data from our experimental OLT-treated mice groups show that these effects were independent of the effects of ventricular remodeling, systolic function, and contractility (+dP/dt, -dP/dt) after a nonreperfused AMI.

CHAPTER 4: Discussion

How inflammation, dependent on the NLRP3 inflammasome, contributes to AMI, cardiac remodeling, and HF progression, is a continuous and complex topic of research. Especially since inflammation has been shown to be both beneficial and detrimental in processes following myocardial injury. To further elucidate the efficacy of a novel targeted anti-inflammatory strategy, this present study was designed to investigate both the role of the NLRP3 inflammasome after a nonreperfused AMI, and the effects that inhibiting NLRP3 could have on blunting aberrant NLRP3 pro-inflammatory signaling following a severe AMI, thereby potentially limiting the pathophysiological processes that occur in ischemic heart failure.

The results of this current study so far have shown that NLRP3 inhibition in OLT-treated mice significantly preserved contractile reserve/ß-adrenergic response, as well as prevented left ventricular diastolic dysfunction in a large nonreperfused anterior AMI, while having no effect on limiting cardiac enlargement (dilatation) and left ventricular systolic dysfunction (reduced LVEF). The majority of these results are in line with numerous past studies that have targeted different levels of the NLRP3 molecular pathway, whether targeting downstream products such as IL-1ß (Abbate et al., 2008), and caspase-1 (Frantz et al., 2003), or the more upstream targets such as P2X7 receptor (Mezzaroma et al., 2011), MyD88 (B. Van Tassell et al., 2011), and the NLRP3 inflammasome (Mezzaroma et al., 2011; Toldo et al., 2019).

As mentioned previously, the findings from a murine ischemia-reperfusion injury model study by Toldo et al. in 2019 confirmed the potential clinical translational value of utilizing OLT1177 as a cardioprotective strategy following myocardial injury. The findings from this ischemia-reperfusion injury model study showed OLT177 having a reducing effect on cardiac damage, as evidenced by limiting infarct size, LV systolic dysfunction, LV diameters, and

caspase-1 activity. This previous study was also key in determining that intraperitoneal injection of OLT1177 reaches maximal efficacy when given within one hour after reperfusion. In light of these results, our study utilized OLT1177 in a long-term and more severe ischemic injury model. We would expect NLRP3 inflammasome activation, oligomerization, and release of pro-inflammatory cytokines/signaling to have already been initiated and propagated by the time OLT1177 diet was administered in our subjects. Thus, focusing on the efficacy of targeting the upstream NLRP3 inflammasome by way of OLT1177 NLRP3 inhibition 1 week after myocardial injury.

One particular study with a similar experimental design and results was conducted in 2014 by Toldo et al. In this study a nonreperfused AMI murine model was also used, along with a mouse monoclonal antibody raised against mouse IL-1ß (10mg/kg) which was injected (i.p.) one week after surgery for 9 weeks/once a week. The main findings from utilizing an IL-1ß blockade strategy showed analogous results in regard to the significant preservation of diastolic function and restoration of contractile reserve, while having no significant effect on cardiac enlargement (Toldo et al., 2019). Where our results differ are on the positive effects that IL-1ß blockade had on preserving systolic function. Possible reasons for this divergence can be attributed to the differences in dosages, bioavailability, and efficacy of each experimental drug. Another possible explanation can be due to differences in targets, with OLT1177 targeting the more upstream NLRP3 inflammasome, whereas the IL-1ß antibody was directed against the more downstream pro-inflammatory IL-1ß cytokine. On that account, it would seem plausible to suggest that 1 week after a nonreperfused AMI, NLRP3 activation, oligomerization, and release of cytokines such as IL-1ß may have already led to an enhanced post-infarction inflammatory response characterized by chronic IL-1ß activity. Hence, the IL-1ß antibody could possibly be

more effective at limiting systolic dysfunction due to targeting chronic IL-1ß activity, which in previous studies has been shown to promote adverse cardiac remodeling and systolic dysfunction (Bujak et al., 2008; Ørn et al., 2012). Nevertheless, without a side-by-side comparison analyzing caspase-1 activity and cytokine levels, it would be difficult to fully ascertain the effectiveness of each drug on systolic function.

Another study that used a nonreperfused AMI murine model was conducted by Marchetti et al. in 2015 (Marchetti et al., 2015). Although this study had a shorter duration, their results after injecting an NLRP3 inhibitor, a small molecule referred to as 16673-34-0 (100mg/kg) once a day for 7 days following AMI surgery, show that the NLRP3 inhibitor, initiated after myocardial ischemia, limited both cardiac enlargement and LV systolic dysfunction. Where our study design and results differ from this study are on the positive effects that 16673-34-0 has on limiting cardiac enlargement and preserving LV systolic function. A possible explanation for this difference can be attributed to the timing of administration, in which 16673-34-0 was applied the same day of the AMI, whereas in our study OLT1177 being applied 1 week after the AMI. Another likely reason can be attributed to the duration of the study. When comparing a 10-week nonreperfused AMI to a 1-week nonreperfused AMI it would be reasonable to expect to see a more a severe form of adverse cardiac remodeling, with higher levels of caspase-1 activity (mRNA synthesis) which according to a previous study by Mezzaroma et al. increases severalfold in the heart 3-7 days after an AMI (Mezzaroma et al., 2011) and higher levels of IL-1ß which has been shown to amplify the inflammatory response leading to higher degrees of apoptosis, LV systolic dysfunction and severe cardiomyopathy in the mouse (Mezzaroma et al., 2011) (B. W. Van Tassell, Seropian, et al., 2013).

This present study had several potential drawbacks and limitations. Some of the more common limitations seen in preclinical studies revolve around the use of mice, such as using only one breed, using only relatively young healthy male mice, and having a small number of subjects. For future studies, performing experiments on mice with other co-morbidities such as diabetes mellitus, obesity, advanced age, or hypertension to simulate the present population most at risk of developing cardiovascular diseases could be a way to limit these drawbacks. Another limitation of this study is the subjective variability in transthoracic echocardiogram measurements of LV dimensions and function.

Some of the more unique limitations that occur in our study are related to the method of oral drug administration. As referenced earlier, our study's experimental drug was admixed into our subjects' diet. With this form of administration potential drawbacks can occur. For example, we noticed that both experimental mice groups during the first two-three weeks consumed a lower amount of food containing OLT1177, which could be a potentially confounding feature of the experiment. One way to address this limitation for future studies would be to implement more precise and accurate drug administration methods, such as oral gavage or intraperitoneal injections, as well as measuring test subjects' blood/plasma regularly to ensure that the appropriate therapeutic range of the experimental drug is being met throughout the study.

Another limitation of this study was not measuring inflammatory cytokine levels as done in previous studies. Although this is a notable limitation, based on our results when compared to findings from previous studies (Marchetti, Swartzwelter, Gamboni, et al., 2018b) (Toldo et al., 2019) we infer that OLT1177 admixed into the experimental groups' diet was effective at inhibiting the NLRP3 inflammasome's activity. Furthermore, our results give us reason to believe that the inhibition of NLRP3 activation and oligomerization would follow and lead to

reduced caspase-1 activity, less IL-1ß and IL-18 released, less pyroptotic cell death, and overall a decrease in sterile inflammatory response. To address this limitation for future studies, mRNA analysis of caspase-1 activity or cytokine levels (IL-1ß or IL-18), whether by Western blot densiometric analysis or ELISA assay, would prove useful in helping to quantify the effects of OLT1177 on post-infarction inflammatory response.

Despite these limitations, the results presented in this study show that NLRP3 inhibition with OLT1177 can restore contractility reserve/ß-adrenergic responsiveness and prevent left ventricular diastolic dysfunction after a large non-reperfused anterior AMI in mice, thereby reducing the risk of developing post-infarct heart failure.

CHAPTER 5: Conclusion

There is currently an urgent need to develop safe and effective therapeutic strategies to prevent or treat heart failure. This need is drastically intensified in patient populations that have a large myocardial infarction, do not receive effective reperfusion therapies in the appropriate therapeutic window of time, as well as in patients with other comorbidities that lessen the effects of reperfusion therapies. Based on the results from this present study and previous ones, reducing the aberrant NLRP3 inflammasome signaling and the resulting exuberant inflammatory response that follows a myocardial injury is a promising strategy. Therefore, these patients who are most at risk of developing post-AMI adverse cardiac remodeling and heart failure would potentially benefit the most from an NLRP3 inhibitor such as OLT177.

Even so, there are currently no targeted anti-inflammatory strategies routinely used for preventing the inflammatory and pathophysiological processes that occur after an acute myocardial infarction and during heart failure. To address this void, studies in the last ten years, such as the CANTOS trial (Ridker et al., 2017), VCU-ART (Abbate et al., 2010), VCU-ART2 (Abbate et al., 2013), and REDHART (B. W. Van Tassell et al., 2017) have provided evidence in support of implementing the concept of utilizing IL-1 blockade to inhibit the NLRP3 mediated inflammatory response, in order to improve the outcomes of patients with severely damaged hearts. With continued efforts, and further elucidation of the mechanisms and inflammatory signaling processes that occur after a myocardial injury, more clinical trials investigating inflammation as a potential target for therapeutic interventions are on their way.

Regarding the future translational value of utilizing OLT1177, one recent study has shown promising anti-inflammatory effects of utilizing OLT1177 and a good safety profile in patients with gout. Additionally, a recently completed phase 1b clinical trial, investigated the

effects of OLT1177 (100mg dapansutrile capsules) in patients with systolic heart failure.

Although the results have not yet been published, if this study was able to confirm a protective

effect brought about by inhibiting the NLRP3 inflammasome, it follows that continued clinical

trials on OLT1177 may be warranted and one day help in preventing and treating heart failure.

REFERENCES

1. Abbate, A. (2017). Why the CANTOS Is a Game Changer in Cardiovascular Medicine. *J Cardiovasc Pharmacol Ä*, *70*(6). www.jcvp.org

2. Abbate, A., Biondi-Zoccai, G. G., & Baldi, A. (2002). Pathophysiologic role of myocardial apoptosis in post-infarction left ventricular remodeling. *Journal of Cellular Physiology*, *193*(2), 145–153. https://doi.org/10.1002/jcp.10174

3. Abbate, A., Kontos, M. C., Grizzard, J. D., Biondi-Zoccai, G. G. L., Van Tassell, B. W., Robati, R., Roach, L. M., Arena, R. A., Roberts, C. S., Varma, A., Gelwix, C. C., Salloum, F. N., Hastillo, A., Dinarello, C. A., & Vetrovec, G. W. (2010). Interleukin-1 Blockade With Anakinra to Prevent Adverse Cardiac Remodeling After Acute Myocardial Infarction (Virginia Commonwealth University Anakinra Remodeling Trial [VCU-ART] Pilot Study). *American Journal of Cardiology*, *105*(10), 1371-1377.e1. https://doi.org/10.1016/j.amjcard.2009.12.059

4. Abbate, A., Salloum, F. N., Vecile, E., Das, A., Hoke, N. N., Straino, S., Giuseppe, G. L., Biondi-Zoccai, Houser, J. E., Qureshi, I. Z., Ownby, E. D., Gustini, E., Biasucci, L. M., Severino, A., Capogrossi, M. C., Vetrovec, G. W., Crea, F., Baldi, A., Kukreja, R. C., & Dobrina, A. (2008). Anakinra, a recombinant human interleukin-1 receptor antagonist, inhibits apoptosis in experimental acute myocardial infarction. *Circulation*, *117*(20), 2670–2683. https://doi.org/10.1161/CIRCULATIONAHA.107.740233

5. Abbate, A., Van Tassell, B. W., Biondi-Zoccai, G., Kontos, M. C., Grizzard, J. D., Spillman, D. W., Oddi, C., Roberts, C. S., Melchior, R. D., Mueller, G. H., Abouzaki, N. A., Rengel, L. R., Varma, A., Gambill, M. L., Falcao, R. A., Voelkel, N. F., Dinarello, C. A., & Vetrovec, G. W. (2013). Effects of interleukin-1 blockade with anakinra on adverse cardiac remodeling and heart failure after acute myocardial infarction [from the virginia commonwealth university-anakinra remodeling trial (2) (vcu-art2) pilot study]. *American Journal of Cardiology*. https://doi.org/10.1016/j.amjcard.2013.01.287

6. Abouzaki, N., & Abbate. (2016). Causes and Prevention of Ventricular Remodeling After MI. *Acc*, *Figure 1*, 1–8.

7. Antman, E. M., Tanasijevic, M. J., Thompson, B., Schactman, M., Mccabe, C. H., Cannon, C. P., Fischer, G. A., Fung, A. Y., Thompson, C., Wybenga, D., & Braunwald, E. (1996). Cardiac-specific troponin I levels to predict the risk of mortality in patients with acute coronary syndromes. *New England Journal of Medicine*, *335*(18), 1342–1349. https://doi.org/10.1056/NEJM199610313351802

8. Aydin, S., Ugur, K., Aydin, S., Sahin, İ., & Yardim, M. (2019). Biomarkers in acute myocardial infarction: Current perspectives. In *Vascular Health and Risk Management* (Vol. 15, pp. 1–10). Dove Medical Press Ltd. https://doi.org/10.2147/VHRM.S166157

9. Azevedo, P. S., Polegato, B. F., Minicucci, M. F., Paiva, S. A. R., & Zornoff, L. A. M. (2016). Cardiac Remodeling: Concepts, Clinical Impact, Pathophysiological Mechanisms and Pharmacologic Treatment. *Arquivos Brasileiros de Cardiologia*, *106*(1), 62–69. https://doi.org/10.5935/abc.20160005

10. Bedard, M., Zaru, O. R., & Embl-ebi, E. B. (2019). Pattern recognition receptors ligands Pattern recognition receptors (PRRs): introduction. *BiteSized Immunology*, 1–2.

11. Benjamin, E. J., Muntner, P., Alonso, A., Bittencourt, M. S., Callaway, C. W., Carson, A. P., Chamberlain, A. M., Chang, A. R., Cheng, S., Das, S. R., Delling, F. N., Djousse, L., Elkind, M. S. V., Ferguson, J. F., Fornage, M., Jordan, L. C., Khan, S. S., Kissela, B. M., Knutson, K. L., … Virani, S. S. (2019). Heart Disease and Stroke Statistics-2019 Update: A Report From the American Heart Association. *Circulation*, *139*(10), e56–e528. https://doi.org/10.1161/CIR.0000000000000659

12. Bhatt, A. S., Ambrosy, A. P., & Velazquez, E. J. (2017). Adverse Remodeling and Reverse Remodeling After Myocardial Infarction. *Current Cardiology Reports*, *19*(8). https://doi.org/10.1007/s11886-017-0876-4

13. Broz, P., & Dixit, V. M. (2016). Inflammasomes: Mechanism of assembly, regulation and signalling. In *Nature Reviews Immunology* (Vol. 16, Issue 7, pp. 407–420). Nature Publishing Group. https://doi.org/10.1038/nri.2016.58

14. Broz, P., Von Moltke, J., Jones, J. W., Vance, R. E., & Monack, D. M. (2010). Differential requirement for caspase-1 autoproteolysis in pathogen-induced cell death and cytokine processing. *Cell Host and Microbe*. https://doi.org/10.1016/j.chom.2010.11.007

15. Bujak, M., Dobaczewski, M., Chatila, K., Mendoza, L. H., Li, N., Reddy, A., & Frangogiannis, N. G. (2008). Interleukin-1 receptor type I signaling critically regulates infarct healing and cardiac remodeling. *American Journal of Pathology*, *173*(1), 57–67. https://doi.org/10.2353/ajpath.2008.070974

16. Burke, A. P., Farb, A., Malcom, G. T., & Smialek, J. E. (2014). *Plaque Rupture and Sudden Death Related Artery Disease*. *281*(10), 921–926.

17. Chen, L., Deng, H., Cui, H., Fang, J., Zuo, Z., Deng, J., Li, Y., Wang, X., & Zhao, L. (2018). Inflammatory responses and inflammation-associated diseases in organs. In *Oncotarget*. https://doi.org/10.18632/oncotarget.23208

18. Chertov, O., Yang, D., Zack Howard, O. M., & Oppenheim, J. J. (2000). Leukocyte granule proteins mobilize innate host defenses and adaptive immune responses. In *Immunological Reviews*. https://doi.org/10.1034/j.1600-065X.2000.17702.x

19. Cleutjens, J. P. M., Kandala, J. C., Guarda, E., Guntaka, R. V., & Weber, K. T. (1995). Regulation of collagen degradation in the rat myocardium after infarction. *Journal of Molecular and Cellular Cardiology*, *27*(6), 1281–1292. https://doi.org/10.1016/S0022-

2828(05)82390-9

20. Cohen, M., Boiangiu, C., & Abidi, M. (2010). Therapy for ST-segment elevation myocardial infarction patients who present late or are ineligible for reperfusion therapy. *Journal of the American College of Cardiology*, *55*(18), 1895–1906. https://doi.org/10.1016/j.jacc.2009.11.087

21. Dagenais, M., Skeldon, A., & Saleh, M. (2012). The inflammasome: In memory of Dr. Jurg Tschopp. *Cell Death and Differentiation*, *19*(1), 5–12. https://doi.org/10.1038/cdd.2011.159

22. De Souza, E. E., Hehnly, H., Perez, A. M., Meirelles, G. V., Smetana, J. H. C., Doxsey, S., & Kobarg, J. (2015). Human Nek7-interactor RGS2 is required for mitotic spindle organization. *Cell Cycle*, *14*(4), 656–667. https://doi.org/10.4161/15384101.2014.994988

23. Dinarello, C. A. (2011). Interleukin-1 in the pathogenesis and treatment of inflammatory diseases. *Blood*. https://doi.org/10.1182/blood-2010-07-273417

24. Duncan, J. A., Bergstralh, D. T., Wang, Y., Willingham, S. B., Ye, Z., Zimmermann, A. G., & Ting, J. P. Y. (2007). Cryopyrin/NALP3 binds ATP/dATP, is an ATPase, and requires ATP binding to mediate inflammatory signaling. *Proceedings of the National Academy of Sciences of the United States of America*, *104*(19), 8041–8046. https://doi.org/10.1073/pnas.0611496104

25. Fieno, D. S., Kim, R. J., Chen, E. L., Lomasney, J. W., Klocke, F. J., & Judd, R. M. (2000). Contrast-enhanced magnetic resonance imaging of myocardium at risk: Distinction between reversible and irreversible injury throughout infarct healing. *Journal of the American College of Cardiology*, *36*(6), 1985–1991. https://doi.org/10.1016/S0735-1097(00)00958-X

26. Franchi, L., Muñoz-planillo, R., & Núñez, G. (2012). Sensing and Reacting to Microbes via the Inflammasomes (NIH Public Access Author manuscript). *Nature Immunology*, *13*(4), 325–332. https://doi.org/10.1038/ni.2231.Sensing

27. Frantz, S., Ducharme, A., Sawyer, D., Rohde, L. E., Kobzik, L., Fukazawa, R., Tracey, D., Allen, H., Lee, R. T., & Kelly, R. A. (2003). Targeted deletion of caspase-1 reduces early mortality and left ventricular dilatation following myocardial infarction. *Journal of Molecular and Cellular Cardiology*. https://doi.org/10.1016/S0022-2828(03)00113-5

28. Freire, M. O., & Van Dyke, T. E. (2013). Natural resolution of inflammation. *Periodontology 2000*. https://doi.org/10.1111/prd.12034

29. Gerber, Y., Weston, S. A., Enriquez-Sarano, M., Berardi, C., Chamberlain, A. M., Manemann, S. M., Jiang, R., Dunlay, S. M., & Roger, V. L. (2016). Mortality Associated with Heart Failure after Myocardial Infarction: A Contemporary Community Perspective. *Circulation: Heart Failure*. https://doi.org/10.1161/CIRCHEARTFAILURE.115.002460

30. Goldfine, A. B., & Shoelson, S. E. (2017). Therapeutic approaches targeting inflammation for diabetes and associated cardiovascular risk. *Journal of Clinical*

Investigation. https://doi.org/10.1172/JCI88884

31. Hawkins, N. M., Petrie, M. C., Jhund, P. S., Chalmers, G. W., Dunn, F. G., & McMurray, J. J. V. (2009). Heart failure and chronic obstructive pulmonary disease: Diagnostic pitfalls and epidemiology. *European Journal of Heart Failure*, *11*(2), 130–139. https://doi.org/10.1093/eurjhf/hfn013

32. He, Y., Zeng, M. Y., Yang, D., Motro, B., & Núñez, G. (2016). NEK7 is an essential mediator of NLRP3 activation downstream of potassium efflux. *Nature*, *530*(7590), 354–357. https://doi.org/10.1038/nature16959

33. Hirayama, D., Iida, T., & Nakase, H. (2018). The phagocytic function of macrophage-enforcing innate immunity and tissue homeostasis. In *International Journal of Molecular Sciences*. https://doi.org/10.3390/ijms19010092

34. Kalkman, E. A. J., Van Suylen, R. J., Van Dijk, J. P. M., Saxena, P. R., & Schoemaker, R. G. (1995). Chronic aspirin treatment affects collagen deposition in non-infarcted myocardium during remodeling after coronary artery ligation in the rat. *Journal of Molecular and Cellular Cardiology*. https://doi.org/10.1006/jmcc.1995.0236

35. Kawaguchi, M., Takahashi, M., Hata, T., Kashima, Y., Usui, F., Morimoto, H., Izawa, A., Takahashi, Y., Masumoto, J., Koyama, J., Hongo, M., Noda, T., Nakayama, J., Sagara, J., Taniguchi, S., & Ikeda, U. (2011). Inflammasome activation of cardiac fibroblasts is essential for myocardial ischemia/reperfusion injury. *Circulation*, *123*(6), 594–604. https://doi.org/10.1161/CIRCULATIONAHA.110.982777

36. Kayagaki, N., Stowe, I. B., Lee, B. L., O'Rourke, K., Anderson, K., Warming, S., Cuellar, T., Haley, B., Roose-Girma, M., Phung, Q. T., Liu, P. S., Lill, J. R., Li, H., Wu, J., Kummerfeld, S., Zhang, J., Lee, W. P., Snipas, S. J., Salvesen, G. S., … Dixit, V. M. (2015). Caspase-11 cleaves gasdermin D for non-canonical inflammasome signalling. *Nature*. https://doi.org/10.1038/nature15541

37. Kelley, N., Jeltema, D., Duan, Y., & He, Y. (2019). The NLRP3 inflammasome: An overview of mechanisms of activation and regulation. In *International Journal of Molecular Sciences*. https://doi.org/10.3390/ijms20133328

38. Lamkanfi, M., & Dixit, V. M. (2014). Mechanisms and functions of inflammasomes. *Cell*, *157*(5), 1013–1022. https://doi.org/10.1016/j.cell.2014.04.007

39. Land, W. G. (2015). The role of damage-associated molecular patterns (DAMPs) in human diseases part II: DAMPs as diagnostics, prognostics and therapeutics in clinical medicine. In *Sultan Qaboos University Medical Journal*.

40. Li, X., Thome, S., Ma, X., Amrute-Nayak, M., Finigan, A., Kitt, L., Masters, L., James, J. R., Shi, Y., Meng, G., & Mallat, Z. (2017). MARK4 regulates NLRP3 positioning and inflammasome activation through a microtubule-dependent mechanism. *Nature*

Communications, *8*(May), 1–13. https://doi.org/10.1038/ncomms15986

41. Lieberman, J., Wu, H., & Kagan, J. C. (2019). Gasdermin D activity in inflammation and host defense. *Science Immunology*, *4*(39), eaav1447. https://doi.org/10.1126/sciimmunol.aav1447

42. Lilly, L. S. (2013). Pathophysiology of heart disease: A collaborative project of medical students and faculty: Fifth edition. In *Pathophysiology of Heart Disease: A Collaborative Project of Medical Students and Faculty: Fifth Edition*.

43. Liu, X., Zhang, Z., Ruan, J., Pan, Y., Magupalli, V. G., Wu, H., & Lieberman, J. (2016). Inflammasome-activated gasdermin D causes pyroptosis by forming membrane pores. *Nature*. https://doi.org/10.1038/nature18629

44. Lohse, M. J., Engelhardt, S., & Eschenhagen, T. (2003). What Is the Role of β-Adrenergic Signaling in Heart Failure? In *Circulation Research*. https://doi.org/10.1161/01.RES.0000102042.83024.CA

45. Lu, A., Magupalli, V. G., Ruan, J., Yin, Q., Atianand, M. K., Vos, M. R., Schröder, G. F., Fitzgerald, K. A., Wu, H., & Egelman, E. H. (2014). Unified polymerization mechanism for the assembly of asc-dependent inflammasomes. *Cell*. https://doi.org/10.1016/j.cell.2014.02.008

46. M. Pfeffer E. Braunwald. (1990). Ventricular Remodeling After Myocardial Infarction Experimental Observations and Clinical Implications. *Circulation Journal*, *81*(4), 1161–1172.

47. M. Tanaka, V. Richard, C. Murry, R. Jennings, Reimer, K. (1993). Superoxide Dismutase Pluse Catalase Therapy Delays neither Cell Death nor the Loss of the TTC Reaction in Experimental Myocardial Infarction in Dogs. *J Mol Cell Cardiol*, *25*, 367–378.

48. Mann, G. H. ad D. L. (2011). Chapter 22. Pathophysiology of Heart Failure. In *Braunwald´s Heart Disease 10th Edition*. https://doi.org/10.1016/B978-1-4557-5134-1.00022-6

49. Mantovani, A., Allavena, P., Sica, A., & Balkwill, F. (2008). Cancer-related inflammation. In *Nature*. https://doi.org/10.1038/nature07205

50. Marchetti, C., Swartzwelter, B., Gamboni, F., Neff, C. P., Richter, K., Azam, T., Carta, S., Tengesdal, I., Nemkov, T., D'Alessandro, A., Henry, C., Jones, G. S., Goodrich, S. A., St. Laurent, J. P., Jones, T. M., Scribner, C. L., Barrow, R. B., Altman, R. D., Skouras, D. B., … Dinarello, C. A. (2018a). OLT1177, a β-sulfonyl nitrile compound, safe in humans, inhibits the NLRP3 inflammasome and reverses the metabolic cost of inflammation. *Proceedings of the National Academy of Sciences of the United States of America*, *115*(7), E1530–E1539. https://doi.org/10.1073/pnas.1716095115

51. Marchetti, C., Swartzwelter, B., Gamboni, F., Neff, C. P., Richter, K., Azam, T., Carta, S., Tengesdal, I., Nemkov, T., D'Alessandro, A., Henry, C., Jones, G. S., Goodrich, S. A., St. Laurent, J. P., Jones, T. M., Scribner, C. L., Barrow, R. B., Altman, R. D., Skouras, D. B., … Dinarello, C. A. (2018b). OLT1177, a β-sulfonyl nitrile compound, safe in humans, inhibits the NLRP3 inflammasome and reverses the metabolic cost of inflammation. *Proceedings of the National Academy of Sciences of the United States of America*, *115*(7), E1530–E1539. https://doi.org/10.1073/pnas.1716095115

52. Marchetti, C., Swartzwelter, B., Koenders, M. I., Azam, T., Tengesdal, I. W., Powers, N., de Graaf, D. M., Dinarello, C. A., & Joosten, L. A. B. (2018). NLRP3 inflammasome inhibitor OLT1177 suppresses joint inflammation in murine models of acute arthritis. *Arthritis Research and Therapy*, *20*(1), 1–11. https://doi.org/10.1186/s13075-018-1664-2

53. Marchetti, C., Toldo, S., Chojnacki, J., Mezzaroma, E., Liu, K., Salloum, F. N., Nordio, A., Carbone, S., Mauro, A. G., Das, A., Zalavadia, A. A., Halquist, M. S., Federici, M., Van Tassell, B. W., Zhang, S., & Abbate, A. (2015). Pharmacologic Inhibition of the NLRP3 Inflammasome Preserves Cardiac Function after Ischemic and Nonischemic Injury in the Mouse. *Journal of Cardiovascular Pharmacology*, *66*(1), 1–8. https://doi.org/10.1097/FJC.0000000000000247

54. Martinon, F., Burns, K., & Tschopp, J. (2002). The Inflammasome: A molecular platform triggering activation of inflammatory caspases and processing of proIL-β. *Molecular Cell*, *10*, 417–426. https://doi.org/10.1016/S1097-2765(02)00599-3

55. Martinon, F., Pétrilli, V., Mayor, A., Tardivel, A., & Tschopp, J. (2006). Gout-associated uric acid crystals activate the NALP3 inflammasome. *Nature*. https://doi.org/10.1038/nature04516

56. Medzhitov, R. (2010). Inflammation 2010: New Adventures of an Old Flame. In *Cell*. https://doi.org/10.1016/j.cell.2010.03.006

57. Meissner, F., Molawi, K., & Zychlinsky, A. (2010). Mutant superoxide dismutase 1-induced IL-1β accelerates ALS pathogenesis. *Proceedings of the National Academy of Sciences of the United States of America*. https://doi.org/10.1073/pnas.1002396107

58. Metz, C. A., Stubbs, D. F., & Hearron, M. S. (1986). Significance of infarct site and methylprednisolone on survival following acute myocardial infarction. *Journal of International Medical Research*. https://doi.org/10.1177/03000605860140s102

59. Mezzaroma, E., Toldo, S., Farkas, D., Seropian, I. M., Van Tassell, B. W., Salloum, F. N., Kannan, H. R., Menna, A. C., Voelkel, N. F., & Abbate, A. (2011). The inflammasome promotes adverse cardiac remodeling following acute myocardial infarction in the mouse. *Proceedings of the National Academy of Sciences of the United States of America*, *108*(49), 19725–19730. https://doi.org/10.1073/pnas.1108586108

60. Mitchell, C., Rahko, P. S., Blauwet, L. A., Canaday, B., Finstuen, J. A., Foster, M. C., Horton, K., Ogunyankin, K. O., Palma, R. A., & Velazquez, E. J. (2019). Guidelines for Performing a Comprehensive Transthoracic Echocardiographic Examination in Adults: Recommendations from the American Society of Echocardiography. *Journal of the American Society of Echocardiography*. https://doi.org/10.1016/j.echo.2018.06.004

61. Mohamed, A. A., Arifi, A. A., & Omran, A. (2010). The basics of echocardiography. *Journal of the Saudi Heart Association*. https://doi.org/10.1016/j.jsha.2010.02.011

62. Muñoz-Planillo, R., Kuffa, P., Martínez-Colón, G., Smith, B. L., Rajendiran, T. M., & Núñez, G. (2013). K+ Efflux Is the Common Trigger of NLRP3 Inflammasome Activation by Bacterial Toxins and Particulate Matter. *Immunity*. https://doi.org/10.1016/j.immuni.2013.05.016

63. Ørn, S., Ueland, T., Manhenke, C., Sandanger, Godang, K., Yndestad, A., Mollnes, T. E., Dickstein, K., & Aukrust, P. (2012). Increased interleukin-1β levels are associated with left ventricular hypertrophy and remodelling following acute ST segment elevation myocardial infarction treated by primary percutaneous coronary intervention. *Journal of Internal Medicine*, *272*(3), 267–276. https://doi.org/10.1111/j.1365-2796.2012.02517.x

64. Ortega-Gómez, A., Perretti, M., & Soehnlein, O. (2013). Resolution of inflammation: An integrated view. In *EMBO Molecular Medicine*. https://doi.org/10.1002/emmm.201202382

65. Pandey, A. K., Duong, T., Swiatkiewicz, I., & Daniels, L. B. (2020). A Comparison of Biomarker Rise in Type 1 and Type 2 Myocardial Infarction. *The American Journal of Medicine*. https://doi.org/10.1016/j.amjmed.2020.02.024

66. Park, S., Juliana, C., Hong, S., Datta, P., Hwang, I., Fernandes-Alnemri, T., Yu, J.-W., & Alnemri, E. S. (2013). The Mitochondrial Antiviral Protein MAVS Associates with NLRP3 and Regulates Its Inflammasome Activity. *The Journal of Immunology*. https://doi.org/10.4049/jimmunol.1301170

67. Pellikka, P. A., Arruda-Olson, A., Chaudhry, F. A., Chen, M. H., Marshall, J. E., Porter, T. R., & Sawada, S. G. (2020). Guidelines for Performance, Interpretation, and Application of Stress Echocardiography in Ischemic Heart Disease: From the American Society of Echocardiography. *Journal of the American Society of Echocardiography*, *33*(1), 1-41.e8. https://doi.org/10.1016/j.echo.2019.07.001

68. Ponikowski, P., Voors, A. A., Anker, S. D., Bueno, H., Cleland, J. G. F., Coats, A. J. S., Falk, V., González-Juanatey, J. R., Harjola, V. P., Jankowska, E. A., Jessup, M., Linde, C., Nihoyannopoulos, P., Parissis, J. T., Pieske, B., Riley, J. P., Rosano, G. M. C., Ruilope, L. M., Ruschitzka, F., … Davies, C. (2016). 2016 ESC Guidelines for the diagnosis and treatment of acute and chronic heart failure. In *European Heart Journal*.

https://doi.org/10.1093/eurheartj/ehw128

69. Prabhu, S. D., Frangogiannis, N. G., Service, M., & Einstein, A. (2017). The Biological Basis for Cardiac Repair After Myocardial Infarction: From Inflammation to Fibrosis. *Circu*, *119*(1), 91–112. https://doi.org/10.1161/CIRCRESAHA.116.303577.

70. R. Lang, L. Badano, V. Mor-Avi, J. Afilalo, A. Armstrong, L. E. et al. (2015). Recommendations for Cardiac Chamber Quantification by Echocardiography in Adults: An Update from the American Society of Echocardiography and the European Association of Cardiovascular Imaging. *Journal of the American Society of Echocardiography*, *28*(1), 1–39.

71. Respress, J. L., & Wehrens, X. H. T. (2010). Transthoracic echocardiography in mice. *Journal of Visualized Experiments*, *39*, 1–4. https://doi.org/10.3791/1738

72. Ridker, P. M., Everett, B. M., Thuren, T., MacFadyen, J. G., Chang, W. H., Ballantyne, C., Fonseca, F., Nicolau, J., Koenig, W., Anker, S. D., Kastelein, J. J. P., Cornel, J. H., Pais, P., Pella, D., Genest, J., Cifkova, R., Lorenzatti, A., Forster, T., Kobalava, Z., … Glynn, R. J. (2017). Antiinflammatory Therapy with Canakinumab for Atherosclerotic Disease. *New England Journal of Medicine*, *377*(12), 1119–1131. https://doi.org/10.1056/NEJMoa1707914

73. Roger, V. L., Go, A. S., Lloyd-Jones, D. M., Benjamin, E. J., Berry, J. D., Borden, W. B., Bravata, D. M., Dai, S., Ford, E. S., Fox, C. S., Fullerton, H. J., Gillespie, C., Hailpern, S. M., Heit, J. A., Howard, V. J., Kissela, B. M., Kittner, S. J., Lackland, D. T., Lichtman, J. H., … Turner, M. B. (2012). Heart disease and stroke statistics-2012 update: A report from the American heart association. *Circulation*. https://doi.org/10.1161/CIR.0b013e31823ac046

74. Sánchez-Fernández, A., Skouras, D. B., Dinarello, C. A., & López-Vales, R. (2019). OLT1177 (Dapansutrile), a Selective NLRP3 Inflammasome Inhibitor, Ameliorates Experimental Autoimmune Encephalomyelitis Pathogenesis. *Frontiers in Immunology*, *10*(November). https://doi.org/10.3389/fimmu.2019.02578

75. Schmid-Burgk, J. L., Chauhan, D., Schmidt, T., Ebert, T. S., Reinhardt, J., Endl, E., & Hornung, V. (2016). A genome-wide CRISPR (clustered regularly interspaced short palindromic repeats) screen identifies NEK7 as an essential component of NLRP3 inflammasome activation. *Journal of Biological Chemistry*. https://doi.org/10.1074/jbc.C115.700492

76. Shao, W., Yeretssian, G., Doiron, K., Hussain, S. N., & Saleh, M. (2007). The caspase-1 digestome identifies the glycolysis pathway as a target during infection and septic shock. *Journal of Biological Chemistry*. https://doi.org/10.1074/jbc.M708182200

77. Shi, J., Zhao, Y., Wang, K., Shi, X., Wang, Y., Huang, H., Zhuang, Y., Cai, T., Wang, F., & Shao, F. (2015). Cleavage of GSDMD by inflammatory caspases determines pyroptotic cell death. *Nature*. https://doi.org/10.1038/nature15514

78. Sigusch, H. H., Campbell, S. E., & Weber, K. T. (1996). Angiotensin II-induced myocardial fibrosis in rats: Role of nitric oxide, prostaglandins and bradykinin. *Cardiovascular Research*. https://doi.org/10.1016/0008-6363(95)00214-6

79. Smale, S. T., & Natoli, G. (2014). Transcriptional Control of Inflammatory Responses. *Cold Spring Harbor Perspectives in Biology*. https://doi.org/10.1101/cshperspect.a016261

80. Stylianou, E. (2019). Epigenetics of chronic inflammatory diseases. *Journal of Inflammation Research*, *12*, 1–14. https://doi.org/10.2147/JIR.S129027

81. Subramanian, N., Natarajan, K., Clatworthy, M. R., Wang, Z., & Germain, R. N. (2013). The adaptor MAVS promotes NLRP3 mitochondrial localization and inflammasome activation. *Cell*. https://doi.org/10.1016/j.cell.2013.02.054

82. Swanson, K. V., Deng, M., & Ting, J. P. Y. (2019). The NLRP3 inflammasome: molecular activation and regulation to therapeutics. In *Nature Reviews Immunology* (Vol. 19, Issue 8, pp. 477–489). Nature Publishing Group. https://doi.org/10.1038/s41577-019-0165-0

83. Takahashi, M. (2019). Role of NLRP3 Inflammasome in Cardiac Inflammation and Remodeling after Myocardial Infarction. In *Biol. Pharm. Bull* (Vol. 518, Issue 4).

84. Thygesen, K., Alpert, J. S., Jaffe, A. S., Simoons, M. L., Chaitman, B. R., White, H. D., Katus, H. A., Apple, F. S., Lindahl, B., Morrow, D. A., Clemmensen, P. M., Johanson, P., Hod, H., Underwood, R., Bax, J. J., Bonow, R. O., Pinto, F., Gibbons, R. J., Fox, K. A., … Wagner, D. R. (2012). Third universal definition of myocardial infarction. *European Heart Journal*, *33*(20), 2551–2567. https://doi.org/10.1093/eurheartj/ehs184

85. Toldo, S., & Abbate, A. (2018). The NLRP3 inflammasome in acute myocardial infarction. In *Nature Reviews Cardiology* (Vol. 15, Issue 4, pp. 203–214). Nature Publishing Group. https://doi.org/10.1038/nrcardio.2017.161

86. Toldo, S., Adolfo, †, Mauro, G., Cutter, Z., Van Tassell, B. W., Mezzaroma, E., Giuseppe, M., Buono, D., Prestamburgo, A., Potere, N., & Abbate, A. (2019). *The NLRP3 Inflammasome Inhibitor, OLT1177 (Dapansutrile), Reduces Infarct Size and Preserves Contractile Function After Ischemia Reperfusion Injury in the Mouse*. www.jcvp.org

87. Toldo, S., Mauro, A. G., Cutter, Z., & Abbate, A. (2018). Inflammasome, pyroptosis, and cytokines in myocardial ischemia-reperfusion injury. *Am J Physiol Heart Circ Physiol*,

315, 1553–1568. https://doi.org/10.1152/ajpheart.00158.2018.-Myocardial

88. Trinczek, B., Brajenovic, M., Ebneth, A., & Drewes, G. (2004). MARK4 Is a Novel Microtubule-associated Proteins/Microtubule Affinity-regulating Kinase That Binds to the Cellular Microtubule Network and to Centrosomes. *Journal of Biological Chemistry*, *279*(7), 5915–5923. https://doi.org/10.1074/jbc.M304528200

89. Van Linthout, S., & Tschöpe, C. (2017). Inflammation – Cause or Consequence of Heart Failure or Both? *Current Heart Failure Reports*, *14*(4), 251–265. https://doi.org/10.1007/s11897-017-0337-9

90. Van Tassell, B., Seropian, I., Toldo, S., Salloum, F., Smithson, L., Varma, A., Hoke, N., Gelwix, C., Chau, V., & Abbate, A. (2011). Erratum: Pharmocologic inhibition of myeloid differentiation factor 88 (MyD88) prevents left ventricular dilation and hypertrophy after experimental acute myocardial infarction in the mouse (Journal of Cardiovascular Pharmacology (2010) 55 (385-390)). *Journal of Cardiovascular Pharmacology*, *57*(2), 272. https://doi.org/10.1097/FJC.0b013e31820a8de0

91. Van Tassell, B. W., Canada, J., Carbone, S., Trankle, C., Buckley, L., Erdle, C. O., Abouzaki, N. A., Dixon, D., Kadariya, D., Christopher, S., Schatz, A., Regan, J., Viscusi, M., Del Buono, M., Melchior, R., Mankad, P., Lu, J., Sculthorpe, R., Biondi-Zoccai, G., … Abbate, A. (2017). Interleukin-1 blockade in recently decompensated systolic heart failure: Results from REDHART (Recently Decompensated Heart Failure Anakinra Response Trial). *Circulation: Heart Failure*. https://doi.org/10.1161/CIRCHEARTFAILURE.117.004373

92. Van Tassell, B. W., Seropian, I. M., Toldo, S., Mezzaroma, E., & Abbate, A. (2013). Interleukin-1β induces a reversible cardiomyopathy in the mouse. *Inflammation Research*. https://doi.org/10.1007/s00011-013-0625-0

93. Van Tassell, B. W., Toldo, S., Mezzaroma, E., & Abbate, A. (2013). Targeting interleukin-1 in heart disease. *Circulation*. https://doi.org/10.1161/CIRCULATIONAHA.113.003199

94. Weisman, H. F., Bush, D. E., Mannisi, J. A., & Bulkley, B. H. (1985). Global cardiac remodeling after acute myocardial infarction: A study in the rat model. *Journal of the American College of Cardiology*, *5*(6), 1355–1362. https://doi.org/10.1016/S0735-1097(85)80348-X

95. Westman, P. C., Lipinski, M. J., Luger, D., Waksman, R., Bonow, R. O., Wu, E., & Epstein, S. E. (2016a). Inflammation as a Driver of Adverse Left Ventricular Remodeling after Acute Myocardial Infarction. *Journal of the American College of Cardiology*, *67*(17), 2050–2060. https://doi.org/10.1016/j.jacc.2016.01.073

96. Westman, P. C., Lipinski, M. J., Luger, D., Waksman, R., Bonow, R. O., Wu, E., & Epstein, S. E. (2016b). Inflammation as a Driver of Adverse Left Ventricular Remodeling after Acute Myocardial Infarction. In *Journal of the American College of Cardiology*. https://doi.org/10.1016/j.jacc.2016.01.073

97. Yancy, C. W., Jessup, M., Bozkurt, B., Butler, J., Casey, D. E., Colvin, M. M., Drazner, M. H., Filippatos, G., Fonarow, G. C., Givertz, M. M., Hollenberg, S. M., Lindenfeld, J., Masoudi, F. A., McBride, P. E., Peterson, P. N., Stevenson, L. W., & Westlake, C. (2016). 2016 ACC/AHA/HFSA Focused Update on New Pharmacological Therapy for Heart Failure: An Update of the 2013 ACCF/AHA Guideline for the Management of Heart Failure. *Journal of the American College of Cardiology*. https://doi.org/10.1016/j.jacc.2016.05.011